

Research article

Development and characterization of chitosan–thyme essential oil nanoemulsion films for active packaging of raw chicken drumsticks

Dipanwita Bhattacharya¹, Dhananjay Kumar¹, Pesingi Pavan Kumar², Arun K. Das^{3,*}, P. K. Nanda³, Annada Das⁴, Saurabh Karunamay¹, Kaushik Satyaprakash², Avanish Singh Parmar⁵ and Anshuman Kumar⁶

¹ Department of Livestock Products Technology, Faculty of Veterinary and Animal Sciences, Banaras Hindu University, Mirzapur 231 001, India

² Department of Veterinary Public Health and Epidemiology, Faculty of Veterinary and Animal Sciences, Banaras Hindu University, Mirzapur 231 001, India

³ Eastern Regional Station, ICAR-Indian Veterinary Research Institute, 37 Belgachia Road, Kolkata 700 037, India

⁴ Department of Livestock Products Technology, Siksha-O-Anusandhan University, Khandagiri, Bhubaneswar 751 030, Odisha, India

⁵ Department of Physics, Indian Institute of Technology (BHU), Varanasi 221 005, India

⁶ Department of Animal Genetics and Breeding, Faculty of Veterinary and Animal Sciences, Banaras Hindu University, Mirzapur 231 001, India

*** Correspondence:** Email: arun.das@icar.org.in; Tel: +919007324343.

Abstract: This study focused on the development and characterization of a bioactive film of chitosan (1.5%, w/v) integrated with a thyme (*Thymus vulgaris*) essential oil nanoemulsion (TNEO). The biopolymer was applied on raw chicken drumsticks to assess its effectiveness in preserving the quality and safety of meat under refrigeration. Gas chromatography–mass spectrometry (GC-MS/MS) analysis of the thyme essential oil identified key bioactive components, *viz.* carvacrol (60.18%), m-cymene (22.93%) and thymol (3.24%). The dynamic light scattering (DLS) assay and transmission electron microscopy (TEM) ensured the successful encapsulation and stability of the nanoemulsion. The infusion of thyme nanoemulsion significantly enhanced the morphological features, UV barrier properties, moisture vapor barrier properties, and flexibility of chitosan film- critical properties, fulfilling the requirements for effective meat packaging. Further, scanning electron microscopy (SEM), Fourier transform infrared spectroscopy (FTIR), X-ray diffraction (XRD), and thermogravimetric

analysis (TGA) were performed to analyze the active biopolymers, which ensured the compatibility between nanoemulsion and chitosan matrix. Notably, the film with 2% TNEO exhibited significant antimicrobial activity against *Staphylococcus aureus* (14.67 ± 0.33 mm) and *Escherichia coli* (12.67 ± 0.33 mm), as measured through zones of inhibition (ZOI), and also antioxidant properties ($40.05 \pm 1.19\%$ reactive scavenging activity). When applied to chicken drumsticks, the 2% TNEO film significantly delayed microbial spoilage, inhibited lipid oxidation, and preserved the color attributes of the meat over a 15-day refrigerated storage period compared to no chitosan and TNEO film. From this study, it is concluded that chitosan-thyme nanoemulsion film can be utilized as a highly promising, green active-packaging solution for extending the shelf-life of raw poultry.

Keywords: nanoemulsion; bioactive; chitosan; antimicrobial; antioxidant; biopreservation

1. Introduction

The increasing demand for minimally processed foods, coupled with consumer concern over synthetic preservatives and plastic packaging, has accelerated interest in natural, biodegradable systems for meat preservation. Essential oils (EOs) extracted from aromatic plants are particularly attractive in this context because of their polyphenolic and terpenoid constituents, which provide both antimicrobial and antioxidant functionality in a single ingredient [1–4]. Among them, thyme essential oil (TEO) from *Thymus vulgaris* L. has gained prominence due to its major components, such as thymol, carvacrol and p-cymene, which are capable of disrupting microbial membranes, leaking cellular contents and retarding lipid and protein oxidation in muscle foods [5–7]. However, the direct addition of EOs to foods is often limited by their hydrophobicity, volatility and intense aroma, which can cause rapid activity loss and undesirable sensory changes in products, such as milk and meat [8]. Recent studies have shown that nanoemulsion-based delivery can overcome many of these constraints by producing sub-100 nm droplets with enhanced physical stability, improved aqueous dispersion and a more controlled release profile of active compounds at food interfaces [9,10]. For example, nanoemulsified thyme or other EOs have been reported to significantly inhibit foodborne pathogens such as *Salmonella enterica*, *Bacillus cereus*, and *Listeria monocytogenes* and delay oxidation in dairy and meat systems while maintaining acceptable sensory quality [11,12].

However, to maximize the preservation potential of essential oil nanoemulsions within complex food matrices such as meat, a protective carrier material that offers both structural stabilization and controlled release of active molecules is essential. In this context, chitosan, a biodegradable and biocompatible polysaccharide derived from chitin, has gained attention due to its film-forming ability, biodegradability, and intrinsic antimicrobial properties [13]. The positively charged amino groups of chitosan, interact with negatively charged microbial cell membranes, inducing cell lysis [14]. Furthermore, chitosan films exhibit excellent gas and moisture barrier properties, making them ideal for meat preservation [15]. Needless to say, chitosan is environmentally friendly and can be a biodegradable packaging alternative to petroleum-based plastics, which often cause environmental pollution and microplastic contamination [16]. Numerous reports have demonstrated that chitosan-based films incorporating plant extracts or EOs can slow microbial growth and oxidative deterioration in poultry, beef and seafood, positioning chitosan as a versatile carrier for nanoencapsulated antimicrobial agents [5,7,17–19]. More recently, chitosan films loaded with thyme essential oil or thyme-based

nanoemulsions explored for meat and fish packaging have shown improved mechanical and barrier properties along with enhanced inhibition of spoilage and pathogenic bacteria [7,17,20]. Nevertheless, the structure–function relationships governing droplet size, film morphology, water resistance, and *in situ* antimicrobial/antioxidant efficacy on whole-muscle poultry cuts remain insufficiently clarified, especially under realistic refrigerated storage conditions [21].

Foodborne pathogenic bacteria such as *Escherichia coli* O157:H7 and *Staphylococcus aureus* are of particular concern in raw meat systems because they can survive refrigeration, produce toxins, and cause severe gastrointestinal illness at relatively low infectious doses [22]. Both organisms are frequently associated with raw or minimally processed animal products and have also been used as target pathogens in challenge studies [23]. For example, Salimnejhad et al. [24] demonstrated that an active peptide (epinecidin-1) markedly reduced inoculated *E. coli* O157:H7 and *S. aureus* in raw milk while maintaining antioxidant capacity and acceptable sensory properties. This highlights the need for packaging systems that can simultaneously control these key pathogens and preserve product quality. On the basis of these findings, there is a clear rationale for designing chitosan-based active films capable of delivering thyme nanoemulsions directly to the surface of poultry meat, where contamination and oxidative reactions initiate.

In this context, the present work aimed to develop and characterize a bioactive chitosan film incorporating a thyme essential oil nanoemulsion (TNEO) and to evaluate its suitability as an active packaging material for raw chicken drumsticks under refrigerated storage. The novelty of this study lies in the integration of a well-characterized TNEO system into a chitosan matrix at graded oil concentrations to systematically relate nanoemulsion properties and film structure to key functional attributes, including mechanical performance, water vapor and moisture barrier behavior, antioxidant capacity, *in vitro* antimicrobial activity against *E. coli* and *S. aureus*, and biodegradability in soil. Unlike previous works that either focused on thyme-oil-loaded films without detailed nanoemulsion characterization or assessed nanoemulsion coatings without comprehensive film property analysis, this study applied the resulting films to a whole-muscle poultry model and monitored their physicochemical quality (pH, TBARS, color) and microbiological safety over a 15-day refrigerated period. Accordingly, the specific objective was to determine whether TNEO-incorporated chitosan films can provide an eco-friendly, multifunctional packaging solution that enhances the microbial safety and oxidative stability of raw chicken drumsticks while reducing the dependence on synthetic preservatives and conventional plastic materials.

2. Materials and methods

2.1. Chemicals and bacterial culture

Thyme (*Thymus vulgaris* L.) essential oil was purchased from Falcon Pvt. Ltd., Karnataka, India. Chitosan (medium molecular weight, 75% deacetylated), Tween 80 (nonionic surfactant), glycerol, acetic acid (glacial, $\geq 99\%$) and other chemicals were procured from Merck, Darmstadt, Germany. Bacteriological media, nutrient broth and phosphate-buffered saline (PBS) were procured from Hi-Media Laboratories Pvt. Ltd., Maharashtra, India. Foodborne pathogens, e.g., *E. coli* (ATCC 25922) and *S. aureus* (ATCC 25923), were procured from the Department of Veterinary Public Health and Epidemiology Laboratory, Faculty of Veterinary and Animal Sciences, Banaras Hindu University,

India, for performing the antibacterial assay. Chicken drumsticks were purchased from a supermarket located in Mirzapur district, India.

2.2. Gas chromatography–mass spectrometry (GC–MS/MS) analysis

The bioactive volatile components of *T. vulgaris* essential oil were identified by a GC-MS triple quadrupole (GC-MS TQ8030, Shimadzu Corp., Japan). Gas chromatography was performed on a Restek Rxi-5ms capillary column (30 m × 0.25 mm) coupled to a GC–MS/MS system operated in Q3 scan mode (3–71 min, scan speed 2500, m/z 40–700). The electron ionization source was set at 70 eV. The oven was programmed from an initial 100 °C, ramped at 3 °C/min to 300 °C, and held at this final temperature for 5 min. The injector temperature was maintained at 250 °C, and the GC–MS/MS interface was held at 300 °C. The samples were injected through an all-glass injector in split mode using helium as the carrier gas at 1 mL/min, with a split ratio of 10:1. Compound identification was based on retention times, fragmentation patterns, and comparisons with reference spectra from the NIST library embedded in the instrument software (version 4.52, Shimadzu Sci, Nakagyoku, Kyoto, Japan). The relative abundance of each constituent in the extract was calculated by peak area normalization and expressed as a percentage of the total ion current. The samples were evaluated three times using the GC–MS/MS method [8].

2.3. Preparation of the thyme nanoemulsion

The process of nanoemulsion formulation was performed according to the methods of Noori et al. [25] with slight modifications. Initially, a coarse oil in water (O/W)-type emulsion was prepared by mixing thyme oil (0.5%, 1% and 2%) with the nonionic surfactant Tween 80 (1%, 2% and 4%, respectively) at a 1:2 ratio in deionized water and centrifuging at 6000 rpm for 10 min using a T18 digital ULTRA-TURRAX® (0003720000) homogenizer (IKA, Staufen, Germany). The coarse emulsion was then converted into a nanoemulsion by ultrasonication for 10 min (20 cycles of 30 s on/30 s off). A probe sonicator (Branson Sonifier SFX250, Brookfield, USA) working at 20 kHz, 30% amplitude and 250 W was used for nanoemulsification. The formulation was stored in an amber-colored reagent bottle and kept in the dark at 4 °C until further use [26].

2.4. Characterization of the thyme nanoemulsion

2.4.1. Determination of the particle size, polydispersity index and zeta potential of the encapsulated essential oil

The mean droplet size of the nanoemulsion (considered as z-average), polydispersity index (PDI, size distribution) and zeta potential (surface charge) were measured by the Dynamic Light Scattering (DLS) assay using Zetasizer Nano-ZS (Malvern Instruments, UK) at 25 ± 1 °C temperature. Deionized water was used to dilute the nanoemulsion until it was no longer opaque. This was done to prevent any adverse dispersion or multiple light scattering of the droplets [8,27].

2.4.2. Transmission electron microscopy (TEM) analysis of the nanoemulsion

Transmission electron microscopy (TECNAI 20G2, THERMO FISHER, Bellaterra Spain), with an acceleration voltage of 200 kV, was performed to determine the morphology and size of the encapsulated essential oil nanodroplets. The sample was diluted with ultrapure water, and a drop of the colloidal suspension (5 μ L) was then placed on a carbon-coated copper grid (200 mesh) and left to dry completely at 25 ± 1 °C. The morphology and size of the nanocapsules were then studied under a transmission electron microscope [28,29].

2.5. Preparation of the bioactive film

The chitosan biopolymer was prepared by an intuitive casting technique with suitable modifications [13,27]. Briefly, 3% (w/v) chitosan powder was dissolved in 1% acetic acid under constant magnetic stirring on a hot plate (800 rpm, 30 °C) for 8 h. Subsequently, 1.5% (w/v) glycerol was added once the solid particles had fully dissolved to enhance the plasticizing effect. Thyme nanoemulsion oil (TNEO) (1%, 2%, and 4%) was added to the filmogenic suspension (1:1) so that the film matrix ultimately contained oil concentrations of 0.5%, 1%, and 2% (w/v) in 1.5% (w/v) chitosan. To mix the nanoemulsion evenly, the suspension was homogenized with a homogenizer (IKA T18, Germany) at 6,000 rpm for 3 min, degassed, and then cast onto sterile, dry glass Petri plates that were 8 inches in diameter. The control film was made without the addition of a nanoemulsion. The filmogenic mixture was then dried in a hot oven at 40 °C for 24 h. The dried films were then peeled off, packaged into a low-density polyethylene (LDPE) film, and kept in a desiccator for conditioning (for at least 24 h) before characterization and application (Figure 1).

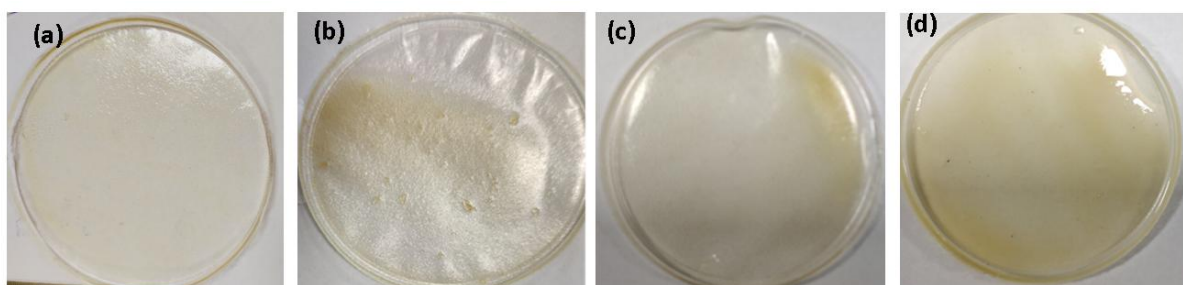


Figure 1. Development of bioactive composite films: (a) chitosan film, (b) chitosan film with 0.5% thyme oil nanoemulsion, (c) chitosan film with 1% thyme oil nanoemulsion, and (d) chitosan film with 2% thyme oil nanoemulsion.

2.6. Characterization of the bioactive film

2.6.1. Scanning electron microscopy (SEM)

The surface morphology and cross-sectional images of each film were analyzed using a scanning electron microscope (ZEISS EV010). Small pieces of the dried films (2–3 mm) were cut and adhered with double-sided carbon tape on copper stubs. The samples were then sprayed with a gold coating

and observed at an accelerating voltage of 10 kV. A cryofractured film part in liquid nitrogen was assessed using cross-sectional analysis [19].

2.6.2. X-ray diffraction (XRD) analysis

The crystalline structure of the film was determined by an X-ray diffractometer (Shimadzu, Kyoto, Japan). Each sample was scanned from 10 to 40° (2θ) at 1° min^{-1} [27].

2.6.3. Attenuated total reflectance-Fourier transform infrared (ATR-FTIR) spectroscopy

The infrared (IR) spectra of the chitosan films were obtained using a Fourier Transform Infrared (FTIR) spectrometer (PerkinElmer, Frontier™, USA) operated in attenuated total reflectance (ATR) mode to analyze the interactions between the thyme essential oil and the chitosan matrix. All the FTIR spectra were obtained at a resolution of 4 cm^{-1} with 16 scans in the spectral range of 4000–400 cm^{-1} [30].

2.6.4. Thermogravimetric analysis (TGA)

The thermal stability of each film sample was checked by heating in a platinum pan from 50 to 600 °C at a rate of $10 \text{ }^\circ\text{C min}^{-1}$ under a nitrogen atmosphere. The degradation temperature was determined according to the peak of the first derivative of the weight with respect to temperature (TGA-50, Shimadzu, Asia Pacific, Pte Ltd., Singapore) [27].

2.6.5. Thickness of the film

The thickness of the film was measured randomly at six different positions. The measurement was taken with a manual micrometer (Mitutoyo No. 293–766, Tokyo, Japan), which had an accuracy of 0.01 mm. The average thickness was subsequently calculated for the film [31].

2.6.6. Film opacity

The film opacity was measured using a UV/VIS spectrophotometer (Spectra Max® M5, Molecular Devices, San Jose, CA, USA) at 600 nm. A rectangular piece of the film was cut and placed into the cuvette cell against an empty sample cell as a blank [13]. The absorbance values were taken from six replicates for each film sample, and the average values were calculated. The opacity of the film was estimated by dividing the mean absorbance value by the thickness (mm).

2.6.7. Mechanical properties of the film

The tensile strength (TS) and elongation at break (EAB) are considered significant parameters for measuring the mechanical strength. These key features were measured by a texture analyzer (ESM 303, MARK-10, USA) according to the ASTM D882-91 principle. A rectangular piece of the film sample (10 mm × 65 mm) was pulled with a head speed of 0.5 mm/s until it broke. The initial distance was fixed at 30 mm between the film ends. Six samples from a single film were analyzed, and the average was computed [32].

2.6.8. Moisture content, water solubility and degree of swelling of the film

The moisture content (MC), water solubility (WS) and degree of swelling (DS) of each film sample were determined [33]. Each film sample was cut into uniform squares (20 mm × 20 mm), weighed (W_1), and then allowed to dry for 24 h at 60 °C until a constant weight (W_2) was reached. Once dried, the weight loss was assessed to calculate the MC, expressed as a percentage of the initial weight of the film. The film sample was then left to soak in 50 mL of distilled water for 24 h at 25 ± 1 °C, after which the weight was measured (W_3). The film residue was dried in an oven at 40 °C for another 24 h prior to determining the final weight (W_4).

$$\text{Moisture content (MC)} = \frac{(W_1 - W_2)}{W_1} \times 100\% \quad (1)$$

$$\text{Water solubility (WS)} = \frac{(W_2 - W_4)}{W_2} \times 100\% \quad (2)$$

$$\text{Degree of swelling (DS)} = \frac{(W_3 - W_2)}{W_2} \times 100\% \quad (3)$$

2.6.9. Water vapor transmission rate (WVTR)

A circular piece of the film was wrapped around a glass beaker containing 15 mL of distilled water. The beaker was placed in a desiccator with silica gel, and a temperature of 25 °C was maintained for 24 h [34]. The weight loss of the experimental beaker was monitored, and the moisture vapor transmission rate was evaluated using the following formula:

$$\text{Water vapor transmission rate (WVTR)} = \frac{\Delta W}{\Delta t \times A} \quad (4)$$

Where the weight difference was depicted as ΔW , the total experimental time (Δt) was 24 h, and A represented the exposed film area.

2.6.10. Antimicrobial characterization of the film

The antibacterial properties of the films were measured against the Gram-negative pathogen *E. coli* (ATCC 25922) and the Gram-positive pathogen *S. aureus* (ATCC 25923) by the disc diffusion test [35]. Using sterile forceps, UV-treated sterile film samples (1 cm² in size) were uniformly plated onto a sterile Muller Hinton agar plate, which was swabbed with 100 µL of an overnight fresh culture (approximately 1 × 10⁶ CFU/mL). The plates were then incubated at 37 ± 1 °C for 24 h, and distinct colony-free zones were observed around the film using a manual micrometre. Growth below the discs was also noted.

2.7. Total phenol content of the bioactive film

The total phenol content of the bioactive film was measured using the Folin–Ciocalteu chromogenic reagent [26,36]. One milligram of each film sample in distilled water was placed on a shaker for one hour, followed by mixing with 1 mL of Folin–Ciocalteu reagent (10%) and allowed to

sit for 2–3 min at 25 ± 1 °C temperature. To this, four millilitres of 7.5% sodium bicarbonate solution were mixed thoroughly and incubated at 25 °C for one hour in the dark. After incubation, the absorbance of each mixture was measured at 760 nm using a spectrophotometer against the standard calibration curve of gallic acid. The results were expressed in micrograms of gallic acid equivalents (GAE)/mg of film. The total phenol content of each film was determined using the following equation (5):

$$\text{TPC (μg GAE/mg film)} = \frac{\text{gallic acid concentration (μg/ml)} \times \text{volume of film extract (ml)}}{\text{weight of film (mg)}} \quad (5)$$

2.8. Antioxidant potential of the film

The DPPH (2,2-diphenyl-2-picrylhydrazyl) radical scavenging assay was used to measure the antioxidant potential of the bioactive film, as described previously [26]. One hundred milligrams of each film sample was immersed in distilled water and incubated in a shaker for 30 min. One mL of each released extract was mixed with 0.5 mL of 0.1 mM methanolic DPPH solution. The mixture was incubated in the dark for 30 min, after which the absorbance at 517 nm was measured using a UV-Vis spectrophotometer (Spectra Max® M5, Molecular Devices, San Jose, CA, USA). The free radical scavenging activity (RSA) of each film was measured as follows:

$$\text{Radical scavenging activity (RSA) \%} = \frac{\text{Abs}_{\text{Control}} - \text{Abs}_{\text{Sample}}}{\text{Abs}_{\text{Control}}} \quad (6)$$

Here, $\text{Abs}_{\text{control}}$ = absorbance of the control, and $\text{Abs}_{\text{sample}}$ = Absorbance of the sample.

2.9. Color analysis of the films

Color measurements were performed using a ColorQuest XE colorimeter (HunterLab, Reston, VA, USA). The instrument was calibrated against a standard white tile ($L^* = 95.78$, $a^* = -0.21$, $b^* = -0.07$) placed in the reflectance port, followed by black trap zeroing. The L^* (brightness), a^* (redness to greenness), and b^* (yellowness to blueness) values of each film were recorded with a colorimeter against a previously calibrated white background. The ΔE value (color difference) was calculated using the following standard formula [26]:

$$\Delta E = \sqrt{\{(\Delta L^*)^2 + (\Delta a^*)^2 + (\Delta b^*)^2\}} \quad (7)$$

Where, ΔE = total color difference, ΔL = lightness difference, Δa = red–green difference, and Δb = yellow–blue difference.

2.10. Sensory evaluation of the films

The sensory attributes (color and aroma) of the bioactive films were assessed using a 9-point hedonic scale, where the highest point (9) represented the ‘extremely liked’ and the lowest point (1) represented the ‘extremely disliked’ [27]. Small circular pieces (3 cm in diameter) of each film were randomly placed in different glass petri plates under daylight, and the temperature was maintained at 25 ± 1 °C. The sensory attributes of the film and any concerns regarding its suitability for food packaging were evaluated in triplicate by 10 trained sensory panellists from the laboratory [37].

2.11. Biodegradation test of the film

The biodegradability of the films was tested by the soil burial method according to the methodology described by Haridevamuthu *et al.* [33] with some modifications. The film samples were cut into uniform squares (20 mm × 20 mm) and weighed (M_i). The earthen pots were subsequently filled with organic soil mixtures collected from the Banaras Hindu University dairy farm, Banaras, Uttar Pradesh, India. Dried film samples were embedded in the soil at a depth of 10 cm and kept under laboratory conditions (25 °C) for 25 days. The wetness of the soil was preserved by spraying 20 mL of tap water every other day. Every five days, the film samples were removed from the soil underneath, and after proper cleaning with soft bristles, the samples were dried (40 °C), and weights were taken (M_f). The soil degradation rate (%) was calculated using the following formula:

$$\text{Soil degradation rate (\%)} = \frac{(M_i - M_f)}{M_f} \times 100 \quad (8)$$

Where, M_i = initial weight (mg) and M_f = final weight (mg) of the film samples.

2.12. Application of bioactive films as packaging materials for chicken drumsticks

The bioactive films were applied to raw chicken drumsticks (each weighing 200 g) to evaluate their shelf life under refrigeration (4 °C) conditions. Chicken drumsticks (approximately 4.8 kg for a single trial) were washed with sterile deionized water and wrapped with UV-treated bioactive films (CS: chitosan film, CS + 1%TNEO: chitosan film with 1% thyme nanoemulsion, CS + 2%TNEO: chitosan film with 2% thyme nanoemulsion), followed by secondary packing in a zip-lock LDPE bag under aseptic conditions. A control (C) meat sample was also studied and packed into a sterile LDPE package without a chitosan film. The drumsticks were periodically assessed under aseptic conditions, and their microbiological, physicochemical, and color properties were evaluated to determine their freshness and shelf life at 4 °C for 15 days.

2.13. Microbiological analysis of chicken drumsticks

A total of 25 g of the meat sample was collected aseptically from the experimental refrigerated drumstick after the film was removed and homogenized using a stomacher bag (Seward, UK) with 225 mL of sterile 0.1% peptone water for 2 min [38]. From this dilution (10^{-1}), 1 mL of solution was transferred into a test tube containing 9 mL of sterile 0.1% peptone water and vortexed for 1 min (10^{-2}). In this way, serial dilutions were prepared aseptically. Appropriate dilutions were used for plating onto specific aseptic agar plates, such as plate count agar for estimating the total viable count (37 °C for 24 h) and psychrophilic bacterial count (4 °C for 7 days). Bacterial colonies were counted from the plates with 30–300 colonies, and the average number of colonies was multiplied by the dilution factor to express the log CFU/g of the sample [39]. Each experiment was performed in triplicate.

2.14. Physicochemical properties

2.14.1. pH

The meat sample (10 g) was homogenized in 90 mL of deionized water by an Ultra-Turrax tissue homogenizer (Model IKA®T 18, Janke and Kenkel, IKA Labor Technik, KG Janke & Kunkel-Str. 10, Staufen) for 2 min, and the pH was measured using a digital pH meter (Hanna HI-98163 Professional Portable Meat pH Meter, Woonsocket, Rhode Island, USA).

2.14.2. Thiobarbituric acid reactive substances (TBARS)

Lipid peroxidation of chicken meat samples was determined by 2-thiobarbituric acid reactive substances (TBARS) analysis [40]. A 10 g meat sample with 25 mL of 20% chilled trichloroacetic acid (TCA) was homogenized for 3 min at 3,000 rpm using an Ultra Turrax tissue homogenizer (Model IKA®T 18, Janke and Kenkel, IKA Labor Technik, KG Janke & Kunkel-Str. 10, Staufen, Germany). The broth was then filtered with Whatman no. 1 filter paper (GE Healthcare, USA). Equal amounts of filtrate and 5 mM thiobarbituric acid (TBA) reagent were correctly mixed in a test tube and dipped into a hot water bath (70 °C for 35 min), followed by immediate cooling under running tap water. The absorbance was recorded against a blank (mixture of TBA and TCA mixture) at 532 nm using an UV-visible spectrophotometer (Spectra Max® M5, Molecular Devices, San Jose, CA, USA). The TBARS value for each sample was assessed by multiplying the absorbance value by 5.2 and reported in mg malonaldehyde per kg (mg MDA/kg) of the meat sample.

2.14.3. Color analysis of the meat samples

Color analysis of the meat samples was performed with a colorimeter (HunterLab, Reston, VA, USA) against a standard white background. The L^* (brightness), a^* (redness to greenness), and b^* (yellowness to blueness) values of each meat sample were measured. The ΔE value (total color difference) was calculated by using the following standard formula [26]:

$$\Delta E = \sqrt{\{(\Delta L^*)^2 + (\Delta a^*)^2 + (\Delta b^*)^2\}} \quad (9)$$

Where, ΔE = total color difference of meat, ΔL = lightness difference of meat, Δa = red–green difference of meat, and Δb = yellow–blue difference of meat.

2.15. Statistical analysis

All the parameters were tested in triplicate, except for the sensory evaluation, where $n = 30$, and the data were compiled and analyzed using SPSS software (version 20, IBM, USA). The storage data were analyzed using two-way ANOVA, with treatment (type of film) and storage time as fixed factors. Tukey's HSD multiple range test was used to compare the mean \pm standard error (SE) values between treatments, and the specific post-hoc test (Tukey's HSD) was used for each data set. For the sensory data of the films, one-way ANOVA was performed for the treatments at each time point, followed by

Tukey's HSD test. Statistical significance was set at $p < 0.05$ (95% confidence level). Graphs were generated using GraphPad Prism software (version 9.0, GraphPad Software, Boston, MA, USA).

3. Results and discussion

3.1. Gas chromatography–mass spectrometry (GC–MS) analysis

Upon GC–MS/MS analysis of the thyme essential oil, the primary bioactive compound identified was phenol, 2-methyl-5-(1-methylethyl)-, and acetate, also known as carvacrol acetate (60.18%), which was one of the total 8 isolated compounds (Supplementary: Figure S1). This monoterpenoid phenolic component has significant antimicrobial and antioxidant properties [41]. Another isolated volatile compound was benzene, 1-methyl-3-(1-methylethyl)-, or m-cymene (22.93%). This terpenoid compound may also demonstrate antibacterial and anti-inflammatory properties [42]. In addition, the other identified compounds were 1, 6-octadien-3-ol, 3,7-dimethyl- or linalool (4.64%), 3-methyl-4-isopropylphenol, p-thymol (3.24%), 3-carene (5.84%), (+)-2-bornanone (1.33%), and eucalyptol (0.86%) [36–38]. These compounds are predominantly monoterpenoids, with a few containing phenol groups. Owing to these biofunctional aromatic components, this bio-oil can function as a natural preservative in food systems. Similar biocomponents were identified by El-Sayed and El-Sayed [17] in *Thymus vulgaris* oil. Variations in the identified phytochemicals from the same essential oil have been noted in different studies, which could be due to differences in species origin, harvesting stage, geo-climatological factors, solvent used and extraction, or distillation protocols [17,43]. Hence, identifying the components of essential oils is a standard and necessary step.

3.2. Characterization of the droplet size, polydispersity index and zeta potential of the nanoemulsion

The average droplet sizes for different TNEO concentrations (0.5%, 1%, and 2%) were 75.39 ± 0.38 nm, 70.39 ± 0.38 nm, and 47.79 ± 0.60 nm, respectively (Table 1). In a previous study, El-Sayed and El-Sayed [17] reported that the mean diameter of a thyme oil emulsion was 52 nm, which aligns with our findings. In fact, the high-pressure deformation forces of an ultrasonicator breakdown coarse oil particles in water-based emulsions into nanosized particles (<100 nm). In this study, the formation of nanosized emulsions was confirmed on the basis of this principle [25,27]. The amphiphilic nature of the TNEO interlinked with Tween 80 (1:2 ratio), which balances both hydrophilic and hydrophobic properties, contributed to particle size reduction, especially when the oil concentration was increased, resulting in smaller droplets; enhanced kinetic stability, surface-to-volume ratio, rheology, and bioavailability; and improved delivery performance. These findings can be attributed to the relatively high surfactant content, which provides sufficient interfacial coverage to lower the interfacial tension and facilitate breakup of the oil phase into a larger number of smaller droplets during emulsification. [26,44].

Table 1. Average diameter (z-average), polydispersity index (PDI) and zeta potential of the thyme oil nanoemulsion (TNEO) at various concentrations.

Thyme oil nanoemulsion (% v/v)	Droplet size (nm)	Poly dispersity index (PDI)	Zeta potential (mV)
TNEO (0.5%)	75.39 ± 0.38 ^C	0.46 ± 0.01 ^C	-13.61 ± 0.63 ^A
TNEO (1%)	70.39 ± 0.38 ^B	0.42 ± 0.01 ^B	-7.08 ± 0.44 ^B
TNEO (2.0%)	47.79 ± 0.60 ^A	0.25±0.00 ^A	-1.93 ± 0.07 ^C

The data are expressed as the means ± standard errors (n = 3), and different letters indicate significant differences (p ≤ 0.05). TNEO-Thyme oil nanoemulsion.

The polydispersity index (PDI) denotes the degree of homogeneity or heterogeneity of the divided droplets in the whole complex of a nanoemulsion. The average PDI values were 0.46 ± 0.01, 0.42 ± 0.01 and 0.25 ± 0.00 for 0.5%, 1% and 2% TNEO, respectively (Table 1). All estimated values were <0.6, indicating moderate homogeneity, except for the 2% nanoemulsion (PDI of 0.25 ± 0.00), which exhibited a uniform droplet size distribution. The higher oil content within the nanoemulsion region, together with the excess surfactant, likely promoted the formation of uniformly sized, well-stabilized droplets and minimized coalescence, which translated into lower PDI values [40]. A comparable PDI value, ranging from 0.2 to 0.5, was observed in copaiba oil nanoemulsions reported by Norcino et al. [27]. In contrast, a narrower PDI value of 0.15 was reported for the *T. vulgaris* EO nanoemulsion, which is attributed to its unimodal particle size distribution while utilizing Tween 80 as a surfactant. [17]. PDI scores closer to 0 indicate a more homogeneous distribution, whereas values approaching 1 suggest a heterogeneous distribution [44].

The zeta potential is another yardstick used to measure the stability of colloidal suspensions by illustrating the surface charge effect and electrostatic repulsion of emulsion droplets [26]. In this study, the zeta potentials of different concentrations of TNEO (0.5%, 1% and 2%) were -13.61 ± 0.63 mv, -7.08 ± 0.44 mv, and -1.93 ± 0.07 mv, respectively (Table 1). These values of electric charge are nearly zero, suggesting the stability of the nanoemulsion with the nonionic surfactant Tween 80 [26,27]. The greater number of negative charges may have contributed to better electric repulsion, which prevented particle aggregation, thus ensuring the stability of the emulsion [27].

3.3. Transmission electron microscopy (TEM) of the nanoemulsion

Transmission electron microscopy (TEM) images of the nanoemulsions at various concentrations (0.5%, 1% and 2%) revealed distinct morphological characteristics (Supplementary Figure S2). The results indicated the presence of irregular, spherical nanosized droplets measuring less than 100 nm, with dimensions ranging from 19 to 62 nm. Correspondingly, an experiment using a 10% thyme oil nanoemulsion demonstrated droplet sizes ranging from 20 to 52 nm, with Tween 80 as the emulsifier [17]. Another study reported a 40-110 nm droplet size range of thyme nanoemulsions prepared with chitosan and sodium tripolyphosphate by TEM [45]. Furthermore, the results of the DLS analysis aligned with those of TEM in terms of droplet diameter, PDI, and zeta potential, exhibiting minimal discrepancies attributed to the processing of various samples for microscopic analysis [28,46]. This interpretation

contrasts with the zeta potential values observed for the 2% nanoemulsion sample, which may be influenced by the sample preparation process, that could expedite the coalescence of small oil droplets.

3.4. Characterization of the bioactive film

3.4.1. Scanning electron microscopy (SEM) of the films

SEM surface micrographs of air-dried chitosan nanoemulsion films and control films without oil are presented in Figure 2 (a-d) to illustrate the organization of the oil droplet distribution, the interaction between the two phases during drying, and the effects of their associations on the mechanical properties and structural orientation of the films [47]. Homogeneous structures, alongside areas with apparent straps and significant corrugations or folds, were observed in the surface morphology of the chitosan film without a nanoemulsion (Figure 2a). The improper crystallization of chitosan particles with additives, degree of deacetylation, and drying atmosphere might be associated with invagination and shrinkage [48,49]. The treated films impregnated with different concentrations of nanoemulsion (CS + 0.5% and CS + 1% TNEO) had homogeneous, compact yet porous structures, indicating the presence of dispersed oil nanodroplets [46,50,51]. A lower concentration of the thyme nanoemulsion in the film matrix resulted in better miscibility and stability, thereby strengthening its controlled-release properties and tensile strength. The presence of micropores is attributed to the migration of oil droplets to the film surface, followed by evaporative loss, leaving the remnants. A few patches and protrusions on the film surfaces indicate aggregation of the nanoemulsion or clumping of the film matrix during the drying process [52].

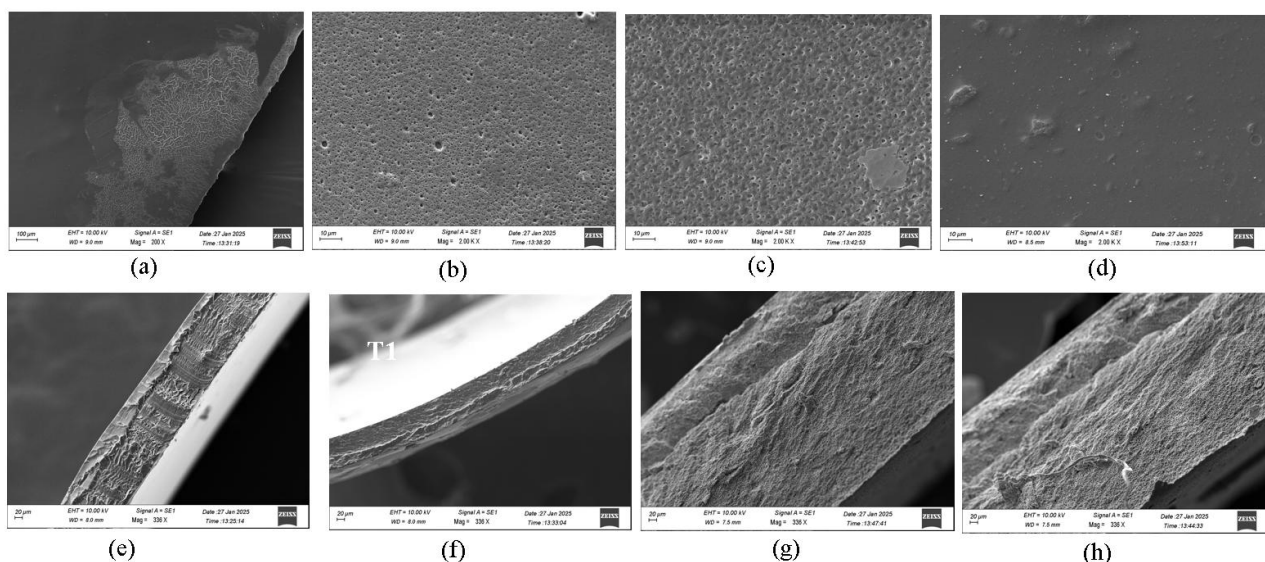


Figure 2. Surface morphology (a, b, c, d) and cross-section (e, f, g, h) study of bioactive films with different concentrations of thyme nanoemulsion; SEM analysis at 10 kV and 336X and 2000X magnifications; (a = CS, b = CS + 0.5% TNEO, c = CS + 1.0% TNEO, d = CS + 2.0% TNEO; e = CS, f = CS + 0.5% TNEO, g = CS + 1.0% TNEO, h = CS + 2.0% TNEO); CS- Chitosan film, TNEO- Thyme nanoemulsion.

When the oil concentration was increased to 2% in the film, the distribution became less uniform with localized aggregation and flocculation, indicating the possibility of phase separation and seepage of the oil to the surface, resulting in a heterogeneous structure [20]. Different studies have shown that the incorporation of essential oil nanoemulsions in different film matrices increases the surface roughness and porosity and results in a heterogeneous structure [50]. In a previous study, Sedláříková et al. [53] reported better interactions between the chitosan matrix and thyme or cinnamon oil nanoemulsion with Tween 80 surfactant, ensuring a compact and homogeneous structure compared with clove oil. Similarly, compared with those of the nonnanoemulsion chitosan film, the cross-sections of the chitosan films (Figure 2, e–h) enriched with various concentrations of oil exhibited dense, stacked, smooth and compact structures with significant cracks.

3.4.2. X-ray diffraction (XRD) study of the film

The existence of crystallographic patterns in the bioactive polymers and the compatibility between chitosan and the thyme oil nanoemulsion were studied and compared using XRD analysis, and the diffractograms are presented in Figure 3a. Herein, the primary diffraction peaks of all the control and treatment films were identified at 2 θ values of 19.96° and 24.46°, with few variations. The characteristic wide peak of the XRD pattern of the pure chitosan film at 20.68° and the sharp peak at 24.42° indicate a semicrystalline structure, which is in agreement with earlier studies [54,55]. Notably, the addition of TNEO to the CS matrix reduced the broadness of the peak intensity at 20°, indicating better compatibility and improved crystallinity due to intermolecular stable hydrogen bonds between the emulsion and the chitosan film. In the case of CS with 0.5% TNEO (T1) and CS with 1.0% TNEO (T2), a few additional narrower peaks were observed, which were attributed to a semicrystalline structure with fewer amorphous zones due to intermolecular spacing in the crystalline lattice. A significant, sharp, and narrow peak was detected at a 2 θ of 24.26° in the case of the 1% oil-incorporated film, which indicates the sharp intensity of the highly crystalline structure of the film compared with the regular structure of the chitosan film. The amalgamation of the TNEO may have improved the crystalline pattern of the CS film, which was reflected in the thermal characterization of the film, as also observed in a previous study [56]. However, in CS with 2.0% TNEO (T3), the diffraction patterns and peaks were similar to those of the pure chitosan film, with an improvement in intensity, thus revealing the formation of hydrogen bonds between the thyme oil and chitosan particles in a compatible way. A previous study reported that copaiba oil in pectin films improved the crystalline properties of pure pectin films when the broader spectrum became narrower and more intense [27].

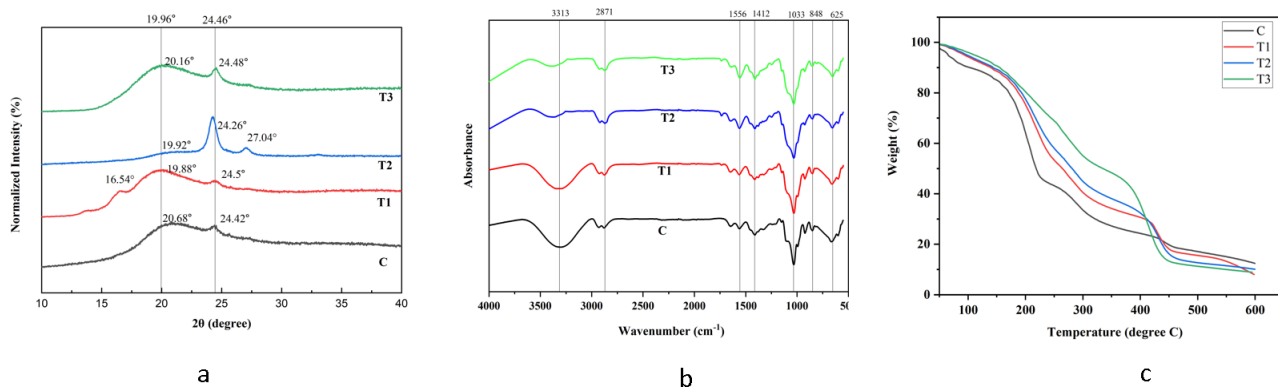


Figure 3. X-ray diffraction (XRD) analysis (a); Fourier transform infrared spectroscopy (FTIR) spectra (b); Thermogravimetric analysis (TGA) curve (c); C-chitosan film, T1-chitosan film with 0.5% thyme oil nanoemulsion, T2-chitosan film with 1% thyme oil nanoemulsion, T3-chitosan film with 2% thyme oil nanoemulsion.

3.4.3. Fourier transform infrared (FTIR) spectroscopy of the film

Fourier transform infrared (FTIR) spectroscopy was conducted to identify the presence of chemical bonds and functional groups within the bioactive film, which was composed of chitosan and thyme oil (Figure 3b). This analysis further elucidates the potential chemical interactions that may modify the orientation of the polysaccharide chains in the pure chitosan film. The spectrum of the neat chitosan film exhibited an infrared peak at 3325-3400 cm^{-1} , which represented -N-H stretching and -O-H stretching, indicating the presence of amine groups as well as alcohol and phenol groups in the chitosan. The peaks highlighted at 2871 cm^{-1} and 2928 cm^{-1} are attributed to the C-H stretching vibrations of the aliphatic hydrocarbons. The presence of aromatic compounds and alkanes with C=C stretches was confirmed by the identified vibration bands at 1412 cm^{-1} , 1556 cm^{-1} and 1650 cm^{-1} . The complex fingerprint region with absorption peaks at 1033 cm^{-1} , 1108 cm^{-1} , and 988 cm^{-1} was due to the presence of C-O stretches with alcohols, carboxylic acids, esters, or ether groups. In addition to these absorption peaks, the spectra of alkyl and aryl halides at 600 cm^{-1} to 900 cm^{-1} also confirmed the presence of chitosan polysaccharide molecules. All these bands confirmed the appearance of hydroxyl groups and amino groups in the chitosan film and their association with the plasticizer glycerol [12,46,57]. An analogous vibrational FTIR spectral range was also reported for chitosan films by Liu *et al.* [46].

Compared with the control, chitosan films containing thyme oil nanoemulsions at various concentrations presented similar infrared spectra, with only minor variations [13,58]. Notably, in the cases of the chitosan film (CS) with 0.5% thyme oil nanoemulsion (T1) and the chitosan film (CS) with 1.0% thyme oil nanoemulsion (T2), the peak at 3313 cm^{-1} in the chitosan film shifted toward higher vibration frequencies, accompanied by a shorter but broader peak. The possible explanations are that the molecular interactions (covalent bonding) between the thyme oil functional groups (hydroxyl) and the chitosan (amine and hydroxyl groups) film matrix that may have left fewer functional groups for absorption [27,46]. Moreover, the widening of the peak intensity ensures the overlapping of multiple peaks in the spectra due to the incorporation of an emulsion containing monoterpenoid phenols (carvacrol, thymol), which have multiple functional groups that differ from those

of chitosan. The addition of thyme oil increased the peak intensity at 2871 cm^{-1} , indicating increased stretching of the -O-H bond due to the presence of sesquiterpenes [58]. The new peak at 1732 cm^{-1} is attributed to the presence of aldehydes and ketones, characterized by C=O stretching, in the treated films. An increase in the transmittance intensities at 1556 cm^{-1} and 1033 cm^{-1} in chitosan film (CS) with 0.5% thyme oil nanoemulsion (T1) and the chitosan film (CS) with 1.0% thyme oil nanoemulsion (T2) highlighted the existence of thyme oil functional groups (aromatic groups, carboxylic acids, ethers, and alcohols) [13,57]. In the fingerprint region, few changes in signature peak intensities confirmed the successful incorporation of the thyme nanoemulsion in the chitosan film matrix, and these changes were significant for the chitosan film (CS) with 0.5% thyme oil nanoemulsion (T1) and the chitosan film (CS) with 1.0% thyme oil nanoemulsion (T2) [58].

3.4.4. Thermogravimetric analysis (TGA) of the films

The thermal stability of the chitosan films containing different concentrations of the thyme nanoemulsion was determined by thermogravimetric analysis (TGA) in the temperature range of 50–600 °C (Figure 3c). Here, the primary degradation peak was identified in the range of 61–115.19 °C for both the control and treatments. The weight reduction (12.46%) at this stage is attributed to evaporative water loss from the chitosan film. In the treatment films, the incorporation of essential oils slowed the weight loss process (7.13%), which could be due to their hydrophobic characteristics [59].

Furthermore, prominent thermal decomposition (45.26%) of the chitosan film was observed between 170.68 and 231.36 °C, indicating the initial degradation of the deacetylated polymeric chains of chitosan and dehydration of the residual solvent. Pyrolysis of the control film was observed at a temperature range of 289.20 to 380.62 °C, facilitating char formation and glycerol decomposition. In the temperature range of 438.44 to 586.83 °C, final degradation with total loss of mass (90.95%) was identified. Similar findings have been reported in different studies [60].

Owing to the inclusion of essential oil, the treated films initially exhibited improved thermal stability compared with the chitosan film, resulting from the compatible dispersion of the oil within the film matrix and compact polymeric chains [7]. Principal decomposition of the bioactive polymer was observed in the thermogram at 165 - 409.58 °C. Compared with that of the control film, the total weight loss of the thyme nanoemulsion-based chitosan films (T1-80.00%, T2-83.58% and T3-90.42%) increased as the concentration of oil increased, and these films were more sensitive at higher temperatures, with a rapid decomposition slope [59,61].

3.5. Thickness and opacity of the film

Thickness is a primary yet essential physical characteristic of a film and is directly correlated with its mechanical strength and water vapor transmission rate [26]. In the present study, the thickness of the control film was $0.091 \pm 0.01\text{ mm}$ (Table 2). This thickness increased significantly ($p < 0.05$) with the addition of stable thyme oil nanoemulsions at varying levels to the film matrix. Increasing the solid content in a chitosan film suspension leads to alterations in the spatial arrangements of the polymeric matrix, and a dense structure is produced [13]. Similar findings were reported by various researchers [12,35,46], who reported that adding essential oil enhances the thickness of the biopolymer.

In addition to the examination of film thickness, the opacity or turbidity of the chitosan film significantly increased ($p < 0.05$) upon incorporation of the essential oil nanoemulsion (Table 2). The

opacity was greater in the film containing 2% emulsion (2.62 ± 0.20) than in the control chitosan film (1.05 ± 0.28). This is likely due to the decreased transmission of UV light through the treated films, which resulted from the uneven distribution of opaque thyme oil emulsion droplets across the surface of the chitosan film, as well as the light-scattering and creaming effects of the dispersed oil particles [30]. Although this property decreases the product's visibility, it effectively preserves the antioxidant characteristics of essential oils that counteract lipid peroxidation and photosensitive reactions within the food system [46,56,62].

3.6. Mechanical properties of the films

Tensile strength (TS) and elongation at break (EAB) are two fundamental parameters utilized to assess the mechanical properties of biopolymers. The tensile strength of the chitosan film began to decrease ($p < 0.05$) after the inclusion of the thyme oil nanoemulsion (Table 2). The primary reason for the decrease in tensile strength is the weaker intermolecular association between the film matrix and the essential oil and the reduction in the cohesive network within the polymer matrix [63]. SEM images also revealed a heterogeneous and rough structure characterized by various flocculants and the coalescence of oil droplets. Additionally, the occurrence of evaporative loss during the drying process and the formation of numerous holes were noted. These features may be linked to characteristics of weakness that contributed to a reduced tensile strength.

Table 2. Physical and mechanical characteristics of thyme oil nanoemulsion (TNEO)-based chitosan films (CSs).

Samples	Thickness (mm)	Moisture Content (%)	Water solubility (%)	Degree of Swelling (%)	Opacity	Tensile Strength (MPa)	Elongation at break (%)	WVTR (g/m ² d)
CS	0.091 ± 0.01^a	27.306 ± 1.31^d	46.556 ± 1.22^d	38.004 ± 1.89^c	1.05 ± 0.28^a	12.56 ± 0.95^e	69.78 ± 1.74^a	2.26 ± 0.36^c
CS + 0.5%	0.127 ± 0.05^b	22.410 ± 0.83^c	35.288 ± 1.302^c	31.408 ± 1.64^c	1.41 ± 0.41^b	9.44 ± 1.37^{bc}	75.38 ± 1.00^b	2.30 ± 0.19^c
CS + 1%	0.193 ± 0.05^c	17.322 ± 1.14^b	18.599 ± 1.38^b	23.778 ± 1.47^b	1.81 ± 0.20^c	7.15 ± 0.93^{ab}	80.70 ± 1.37^b	1.95 ± 0.23^b
CS + 2%	0.224 ± 0.10^d	9.138 ± 0.78^a	13.746 ± 1.02^a	14.201 ± 0.89^a	2.62 ± 0.20^d	4.84 ± 0.92^a	91.77 ± 1.36^c	1.51 ± 0.34^a

The data are expressed as the means \pm standard errors ($n = 3$), and superscripts with different letters indicate significant differences ($p \leq 0.05$) within a column; CS-chitosan film; TNEO-Thyme oil nanoemulsion; WVTR- water vapor transmission rate.

The EAB of the chitosan films with various concentrations of nanoemulsion differed significantly ($p < 0.05$) from that of the neat chitosan film (Table 2), with EAB values reaching $91.77 \pm 1.36\%$ in the film with 2% TNEO. This increase in the stretchability of the bioactive film could be due to the presence of the hydroxyl group of the thyme essential oil nanoemulsion, which may enhance the plasticizing effect of the film [28]. This mechanical property is advantageous for wrapping food products. In one study, when large oil droplets were divided into nanodroplets with a stabilizer, their plasticizing effect improved [64]. In addition, oil nanoemulsions loosen the internal hydrogen bonds between the polymer chains, enhancing mobility and increasing stretchability [57]. A similar result

was reported by Al-Hilifi et al. [65], in which increasing the concentration of ginger essential oil improved the stretchability of the chitosan film.

3.7. Moisture content (MC), water solubility (WS), and swelling index (SI) of the film

The moisture content (MC), water solubility (WS), and swelling index (SI) are critical factors in determining the effectiveness of food packaging for commercial applications. In the present study, the MC and WS of the films decreased significantly ($p < 0.05$) when the thyme oil nanoemulsion was incorporated into the chitosan film at different concentrations (Table 2). The moisture content decreased from $27.306 \pm 1.31\%$ to $9.138 \pm 0.78\%$, and the water solubility decreased from $46.556 \pm 1.22\%$ to $13.746 \pm 1.02\%$ in the chitosan films upon the addition of 2% TNEO. The decreased water solubility could be due to the hydrophobic nature of the thyme essential oil, which forms covalent linkages and hydrogen bonds with the chitosan film matrix, leaving very few free hydrogen groups available to bind with water molecules [63]. These reduced properties of the film align with the development of a food packaging material that maintains food integrity and exhibits improved water resistance [30]. This observation was confirmed by various research findings, in which the addition of hydrophobic essential oil reduced the moisture content and solubility of chitosan films in water [5,66].

Comparative assessments of the swelling indices of the films revealed noteworthy distinctions ($p < 0.05$) between the control film and the films with 1% and 2% TNEO (Table 2). Owing to the hydrophobicity of the thyme nanoemulsion, a lesser degree of swelling was observed in the bioactive polymer [30]. These characteristics are essential for guaranteeing the long-term stability of biopolymers, which are particularly suitable for applications in the food packaging industry.

3.8. Water vapor transmission rate (WVTR) of the film

The water vapor transmission rate (WVTR) of the chitosan film was evaluated to assess its environmental compatibility with the food matrix (Table 2). The WVTR of CS with 0.5% TNEO was greater ($2.30 \pm 0.19 \text{ g/m}^2 \text{ d}$) than that of the pure chitosan film ($2.26 \pm 0.36 \text{ g/m}^2 \text{ d}$), and as the concentration of nanoemulsion increased, the WVTR decreased in the treated films. The increased WVTR in the chitosan film with the 0.5% nanoemulsion is likely due to the irregular distribution of nanodroplets and the subsequent volatilization of oil, which creates microscopic holes in the film surface [48]. A chitosan film with a higher concentration of thyme essential oil exhibited better structural cohesiveness due to intermolecular interactions, thereby improving the water vapor barrier properties [26]. Such a lower WVTR in food packaging is one of the most desirable characteristics in terms of shelf-life extension [31].

3.9. *In vitro* antibacterial efficacy test of the biopolymers against *E. coli* and *S. aureus*

The antimicrobial properties of the pure chitosan film and thyme nanoemulsion-based bioactive films are detailed for Gram-negative (*E. coli* ATCC 2592) and Gram-positive (*S. aureus* ATCC 25923) bacteria in Table 3. Here, the zone of inhibition was enhanced in a dose-dependent manner for both organisms. The chitosan film (CS) and the film with 0.5% TNEO did not show any clear inhibition zones against either bacterial strain. However, no growth was detected below the film discs, confirming their bacteriostatic effect [27]. The largest inhibition zone was observed against *S. aureus* in the

chitosan film with 2% TNEO (14.67 ± 0.33 mm), along with an apparent zone diameter of 12.67 ± 0.33 mm against *E. coli*. Similar antibacterial properties of chitosan films infused with thyme oil have been reported in the literature, highlighting the superior antimicrobial effectiveness of thyme essential oil [67]. The inhibition zones showed reduced clarity during the antimicrobial assessment of the thyme oil nanoemulsion in the chitosan films, which might be due to entrapment of the nanoemulsion within the film matrix in a preferred manner, leading to sustained release upon contact with the food matrix [27]. As shown in Table 3, the chitosan film infused with the nanoemulsion demonstrated significantly greater effectiveness against Gram-positive bacteria. This increased sensitivity may be attributed to the presence of polyphenols and terpenoid compounds in the thyme oil nanodroplets, which can disrupt bacterial cell membranes, leading to cell lysis. In contrast, Gram-negative bacteria possess a complex lipopolysaccharide membrane structure that inhibits the easy diffusion of bioactive compounds [58].

Table 3. Antibacterial sensitivity testing of chitosan (CS) films with different concentrations of thyme oil nanoemulsion (TNEO).

Antimicrobial activity of bioactive films	Zone of inhibition (mm) against <i>Escherichia coli</i> (ATCC 25922)	Zone of inhibition (mm) against <i>Staphylococcus aureus</i> (ATCC 25923)
CS	10.00 ± 0.00^A	10.00 ± 0.00^A
CS + 0.5% TNEO	10.00 ± 0.00^A	10.00 ± 0.00^A
CS + 1% TNEO	10.83 ± 0.33^A	11.67 ± 0.33^B
CS + 2% TNEO	12.67 ± 0.33^B	14.67 ± 0.33^C

The data are expressed as the means \pm standard errors ($n = 3$), and superscripts with different letters indicate significant differences ($p \leq 0.05$) in a column. CS-chitosan film; TNEO-Thyme oil nanoemulsion.

3.10. Total phenol content and antioxidant activity of the biopolymers

The total phenol content reflects the potential antioxidant activity of the biopolymers. As depicted in Table 4, the chitosan film had the minimum total phenolic content of 0.71 ± 0.02 μ g gallic acid/mg of film, which increased when the thyme nanoemulsion was added. The highest total phenol content (12.98 ± 0.52 μ g GAE/mg of film) was observed for the film sample infused with a 2% thyme oil nanoemulsion. The polyphenols found in the thyme essential oils significantly ($p < 0.05$) increased the total phenolic content in the treated films. In contrast, the control film, which does not contain phenol, presented a minimal total phenolic content, possibly due to its susceptibility to chromogen formation from nonphenolic compound fragments within the chitosan matrix [36].

The antioxidant capacity is a significant functional property that directly complements the antimicrobial activity of bioactive films. The DPPH (2,2-diphenyl-2-picrylhydrazyl) assay is the most widely used method for assessing free radical scavenging activity. In the present study, the electron-donating power or free radical-scavenging activity was greater in the chitosan film containing the 2% thyme oil nanoemulsion ($40.07 \pm 4.21\%$) than in the other films (Table 4). As the oil concentration increased, the radical-scavenging power of the chitosan film also significantly improved ($p < 0.05$). Our findings are in tandem with those of various studies [33,68], in which the incorporation of thymol increased the antioxidant power of the chitosan film.

Table 4. Antioxidant capacity of the thyme oil nanoemulsion-based chitosan films.

Antioxidant activity of bioactive films	DPPH (2,2-diphenyl-2-picrylhydrazyl) assay (Radical scavenging activity %)	Total phenol content (µg Gallic acid/mg)
CS	7.03 ± 0.97 ^A	0.71 ± 0.02 ^A
CS + 0.5% TNEO	17.13 ± 0.68 ^B	3.48 ± 0.10 ^B
CS + 1% TNEO	30.66 ± 0.79 ^C	8.83 ± 0.20 ^C
CS + 2% TNEO	40.05 ± 1.19 ^D	12.98 ± 0.52 ^D

The data are expressed as the means ± standard errors (n = 3), and superscripts with different letters indicate significant differences (p ≤ 0.05) in a column. CS-chitosan film; TNEO-Thyme oil nanoemulsion.

3.11. Instrumental color profile and sensory scores of the films

The effects of adding a thyme oil nanoemulsion to chitosan films on their color properties and sensory properties were thoroughly analyzed (Table 5), as these elements are essential for consumer acceptance. The lightness decreased from 77.30 ± 1.00 in the chitosan film (without TNEO) to 46.10 ± 2.41 in the CS with 2.0% TNEO, indicating significant differences (p < 0.05). A reduction in the brightness of the treated films may have resulted from the light absorption characteristics of the biomolecules present in the essential oil nanoemulsion, which can increase the opacity of the film [30]. This property although decreases the product's visibility, effectively protects food nutrients from lipid peroxidation and photosensitive reactions [69]. The incorporation of a thyme oil nanoemulsion into a chitosan film enhanced the red hue, with the most pronounced increase observed in the film with 2% TNEO [29]. The yellowness of the chitosan film increased (p > 0.05) with the addition of the thyme oil nanoemulsion at various concentrations. Notably, the film containing 2% essential oil presented the most pronounced coloration and differed significantly (p < 0.05) from the other films. The intrinsic yellowness of thyme oil significantly enhances the yellow coloration of a film during the drying process [67]. The incorporation of 1% and 2% oil emulsions significantly increased the colorimetric profile difference (ΔE) in the chitosan film (p < 0.05), which may vary with the type and concentration of essential oils [26].

The sensory evaluation of biopolymers was conducted to gain insights into consumer preferences and to determine the suitability of the developed biopolymers for future food packaging applications [27]. The sensory scores for the color attributes did not significantly differ (p > 0.05) among the chitosan bioactive films, with up to 1% incorporation of the thyme oil nanoemulsion (Table 5). The CS + 2% TNEO sample differed significantly (p < 0.05) from the control sample, with a lower value. This film received a 'slightly liked' rating from the panellists regarding its color. The higher scores obtained for the control film may be indicative of superior transparency, a desirable characteristic of packaging materials that effectively communicate with consumers. In addition, aroma, which is another essential attribute significantly differed (p < 0.05) across the oil concentrations added to the films. The highest average aroma score was 8.17 ± 0.16 for the chitosan film, which signifies 'mostly liked', where a 1% essential oil nanoemulsion was included [27]. The addition of a nanoemulsion of essential oil may suppress the strong pungency of crude essential oil, maintaining volatile components with an acceptable fragrance. In contrast, the panellists neither liked nor disliked the control film, with an average hedonic rating of 5 points, which might be due to the fishy odor of chitosan.

Table 5. Color profile and sensory scores of the thyme oil nanoemulsion-based chitosan films.

Treatments	<i>L</i> * value	<i>a</i> * value	<i>b</i> * value	ΔE value	Color	Aroma
CS	77.30 ± 1.00 ^c	0.55 ± 0.23 ^b	7.36 ± 1.50 ^a	20.98 ± 1.46 ^a	6.91 ± 0.32 ^b	5.29 ± 0.15 ^a
CS + 0.5% TNEO	73.68 ± 0.86 ^c	0.52 ± 0.19 ^b	10.27 ± 0.65 ^a	23.71 ± 1.15 ^a	6.96 ± 0.09 ^b	6.79 ± 0.27 ^b
CS + 1% TNEO	61.73 ± 1.38 ^b	1.05 ± 0.14 ^a	10.93 ± 1.76 ^a	35.19 ± 1.14 ^b	6.61 ± 0.07 ^{ab}	8.17 ± 0.16 ^c
CS + 2% TNEO	46.10 ± 2.41 ^a	0.50 ± 0.25 ^c	27.71 ± 1.87 ^b	58.55 ± 0.91 ^c	6.03 ± 0.15 ^a	6.18 ± 0.27 ^{ab}

The data are expressed as the means ± standard errors (n = 3), and superscripts with different letters indicate significant differences ($p \leq 0.05$) in a column. CS-chitosan film; TNEO-Thyme oil nanoemulsion; L^* = lightness, a^* = redness/greenness, b^* = yellowness ΔE = total color change.

3.12. Biodegradability test

A soil degradation assessment of bioactive films in a natural environment was conducted over 25 days, with measurements taken every 5 days. A consistently significant difference ($p < 0.05$) was obtained between the pure chitosan film and the treatments. The pure chitosan film demonstrated a significant degradation rate of $71.93 \pm 0.78\%$ at the end of the experiment. In contrast, the soil degradation rates for CS + 0.5% TNEO, CS + 1% TNEO, and CS + 2% TNEO were considerably lower, at $55.28 \pm 0.64\%$, $37.37 \pm 0.91\%$, and $31.21 \pm 0.39\%$, respectively, during the same experimental period (Supplementary Figure S3). The neat chitosan film swelled rapidly due to its hydrophilicity, thereby initiating enzymatic degradation by soil microorganisms. On the other hand, incorporating essential oil nanodroplets slowed the degradation rate of the hydrophilic chitosan film. In fact, nano-oil molecules interact with the entire chitosan film matrix in a compact manner with different intermolecular associations, which reduces the permeation of water [33]. The slowed decomposition could also be attributed to the antimicrobial properties of thyme essential oil, a desirable feature for packaging muscle foods. Nonetheless, all the biopolymers were proven to be biodegradable, resulting in less environmental pollution. Related findings have revealed the biodegradable nature of chitosan films supplemented with various additives [70].

3.13. Application of films in a meat model system

In this experiment, four sample groups were analyzed over a 15-day storage period under refrigerated conditions: one group contained chicken drumsticks without any primary wrapping of chitosan film (C), another group contained chitosan film (CS), and the remaining two groups were wrapped with chitosan films loaded with either 1% or 2% thyme oil nanoemulsion (Figure 4). LDPE was used as secondary packaging for each sample group. Each experiment was conducted in triplicate.

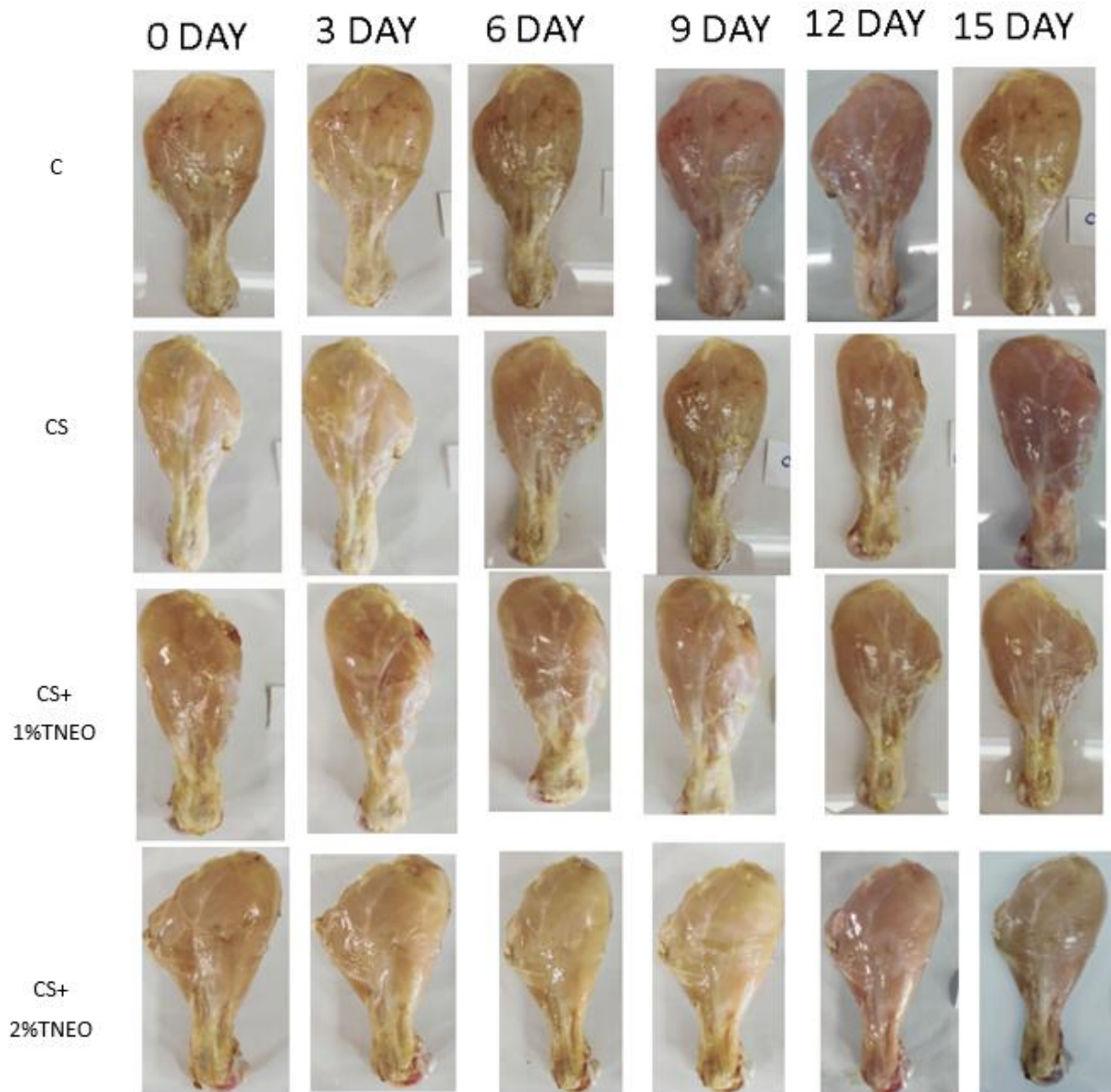
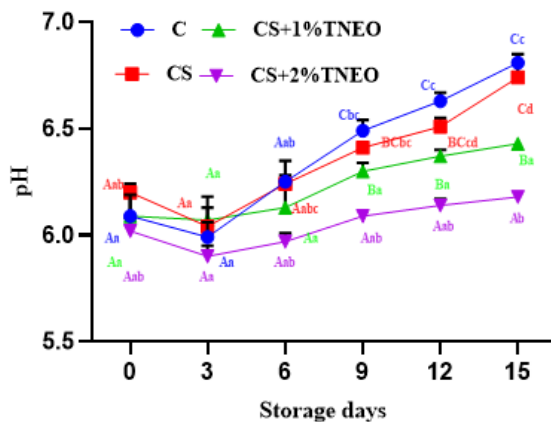


Figure 4. *In vitro* study of bioactive films with different concentrations of thyme oil nanoemulsion (TNEO) on chicken drumsticks under refrigerated storage. C = chicken drumstick without any wrapping; CS = chicken drumstick wrapped with chitosan film (CS); CS + 1% TNEO = chicken drumstick wrapped with CS with a 1% thyme oil nanoemulsion; CS + 2% TNEO = chicken drumstick wrapped with a 2% thyme nanoemulsion.

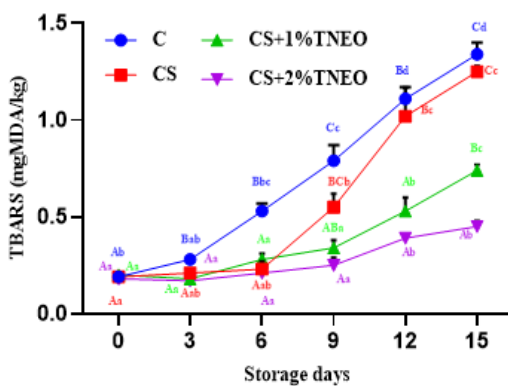
3.13.1. pH

The measurement of pH serves as a critical and straightforward indicator of meat quality degradation, primarily reflecting microbial spoilage and autolytic processes. As illustrated in Figure 5a, the pH of the control sample increased markedly from 6.09 ± 0.10 on day 0 to 6.95 ± 0.04 by day 15, surpassing the regulatory limit of 6.4 for spoiled chicken meat after day 6. All the treatments initially resulted in a slight decrease in pH, a phenomenon often attributed to the postmortem accumulation of

lactic acid from anaerobic glycolysis [51]. However, a significant difference ($p < 0.05$) between the treated samples and the sample containing only the chitosan film (CS) emerged from day 9 onward. While the pH of sample C increased steeply, samples wrapped with bioactive films, particularly CS + 1% TNEO and CS+2% TNEO, demonstrated a markedly slower rate of increase. In CS with 2% TNEO, the pH decreased from 6.02 ± 0.06 to 5.97 ± 0.04 by day 6, before increasing to only 6.18 ± 0.02 by day 15—a value still within the safe limit. This superior performance is likely due to the controlled release of the thyme nanoemulsion from the chitosan film, which effectively delayed microbial proliferation.



(a)



(b)

Figure 5. (a) pH estimation and (b) TBARS estimation of chicken drumsticks under refrigeration for 15 days. C = chicken drumstick without any wrapping; CS = chicken drumstick wrapped with chitosan film; CS + 1% TNEO = chicken drumstick wrapped with 1% thyme nanoemulsion-loaded chitosan film; CS + 2% TNEO = chicken drumstick wrapped with 2% thyme nanoemulsion-loaded chitosan film.

The efficacy of the chitosan matrix itself was evident, as the CS sample (chitosan-only film) also showed comparable preservative effects. The overarching mechanism for the increase in pH in spoiled

meat is the accumulation of basic nitrogenous compounds, such as ammonia and amines, resulting from bacterial decomposition of proteins and endogenous enzyme activity [31]. The thyme nanoemulsion, which is rich in antimicrobial polyphenols such as carvacrol and thymol, directly counteracts this effect by suppressing the spoilage microbiota [58]. Consequently, the 2% nanoemulsion-based chitosan film effectively reduced the rate of pH increase, ensuring an extended shelf-life of 15 days. These findings align with previous work, such as that of Amiri et al. [44], who reported similar pH stabilization and freshness preservation in ground beef using a *Zataria multiflora* nanoemulsion-based starch film.

3.13.2. Thiobarbituric acid reactive substances (TBARS)

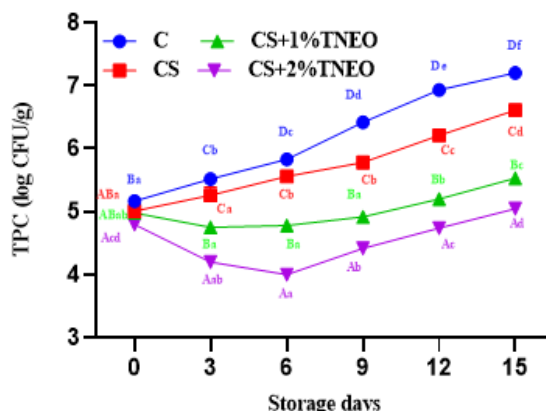
To assess the progression of lipid oxidation, thiobarbituric acid reactive substances (TBARS) were measured, and secondary byproducts such as malondialdehyde (MDA) were quantified. The drumstick sample, without chitosan packaging (C), presented a rapid and significant ($p < 0.05$) increase in TBARS from day 3 onward, reaching 1.34 ± 0.06 mg MDA/kg by day 15, far exceeding the accepted spoilage threshold (Figure 5b). In contrast, all the chitosan-based treatments significantly delayed lipid oxidation. This protective effect is attributed to the dual function of the film as a physical barrier against oxygen and light [56] and, in the case of CS with 1% TNEO and CS with 2% TNEO, as a reservoir of potent antioxidants from the thyme essential oil nanoemulsion. The efficacy of this system was evident, as the TBARS values for CS with 1% TNEO and CS with 2% TNEO were not significantly different ($p > 0.05$) for most of the storage period. Notably, the CS with 2% TNEO sample maintained a low value of 0.45 ± 0.03 mg MDA/kg on day 15, which was well below the 0.6 mg MDA/kg safety limit for raw meat [44,51].

The composition of the essential oil, specifically its bioactive compounds such as thymol and carvacrol, plays a critical role in neutralizing free radicals and chelating pro-oxidant metals [25,71]. The nanoemulsion-loaded films enhanced the stability and consistent release of these compounds, providing sustained protection. This finding is consistent with the work of Huang et al. [72], who successfully retarded oxidative damage in chicken meat using a chitosan coating incorporating a rosemary extract nanoemulsion, confirming the general effectiveness of this delivery strategy for natural antioxidants in meat preservation.

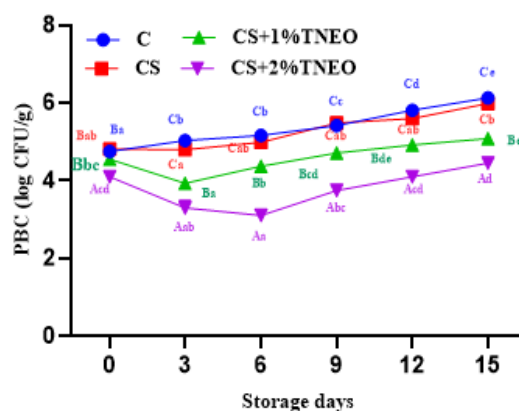
3.14. Microbiological characteristics

The antimicrobial efficacy of the chitosan-based films and thyme nanoemulsion-based chitosan films was evaluated by monitoring the total plate count (TPC) and psychrophilic bacterial count (PBC) over 15 days of storage (Figure 6a and 6b). The TPC of the control sample progressively increased, increasing from 5.17 ± 0.08 to 7.20 ± 0.02 log CFU/g and exceeding the permissible limit for spoilage (6 log CFU/g) by day 9. In contrast, all the active treatments (CS, CS+1% TNEO, and CS+2% TNEO) resulted in significant antimicrobial activity ($p < 0.05$), maintaining lower microbial counts throughout the storage period. The TPC values for CS+1% TNEO and CS+2% TNEO were 4.98 ± 0.04 log CFU/g and 4.80 ± 0.02 log CFU/g, respectively, on day 0 and reached 5.53 ± 0.05 log CFU/g and 5.05 ± 0.03 log CFU/g, respectively, on the 15th day, with a significant difference ($p > 0.05$) from day 3 onward. The 2% thyme nanoemulsion-based chitosan film was the most effective, restricting the TPC to 5.05 ± 0.03 log CFU/g on day 15—a value still within the safe consumption limit. This superior

performance is attributed to the gradual and sustained release of antimicrobial polyphenols and terpenoids from the nanoemulsion, which disrupts bacterial cell membranes and interferes with enzymatic systems, leading to cell death [13,19].



(a)



(b)

Figure 6. Microbiological analysis of chicken drumsticks stored at refrigeration for 15 days: (a) total plate count (TPC) and (b) psychrophilic bacterial count (PBC). C = chicken drumstick without any wrapping; CS = chicken drumstick wrapped with chitosan film; CS + 1% TNEO = chicken drumstick wrapped with 1% thyme nanoemulsion-loaded chitosan film; CS + 2% TNEO = chicken drumstick wrapped with 2% thyme nanoemulsion-loaded chitosan film.

The chitosan-only film (CS) effectively delayed spoilage until day 12, demonstrating the inherent antimicrobial activity of the polycationic amine groups of chitosan, which disrupt negatively charged microbial cell membranes [71]. Nevertheless, its limited efficacy highlights the necessity of incorporating potent essential oils, such as thyme oil, to achieve prolonged preservation. These results align with findings of Wang et al. [51], who reported comparable shelf-life extensions for mutton using thyme-embedded composite films.

A similar trend was observed for PBC, which are particularly challenging owing to their Gram-negative, lipopolysaccharide-rich cell walls that confer inherent resistance. The PBC in chicken drumsticks without chitosan film (C) increased to 6.13 ± 0.04 log CFU/g by day 15. Notably, compared with the non-chitosan-packed sample, the sample with 2% TNEO treatment achieved a 1.68 log CFU/g reduction in PBC. This highlights the potency of lipophilic compounds such as thymol and carvacrol in thyme oil, which can disorganize the outer membrane, penetrate the cytoplasm, and collapse the proton motive force, ultimately causing cell death [18,73]. The successful suppression of psychrophiles aligns with studies on cinnamon and green cardamom essential oil coatings, reinforcing the broad applicability of this strategy [19,71].

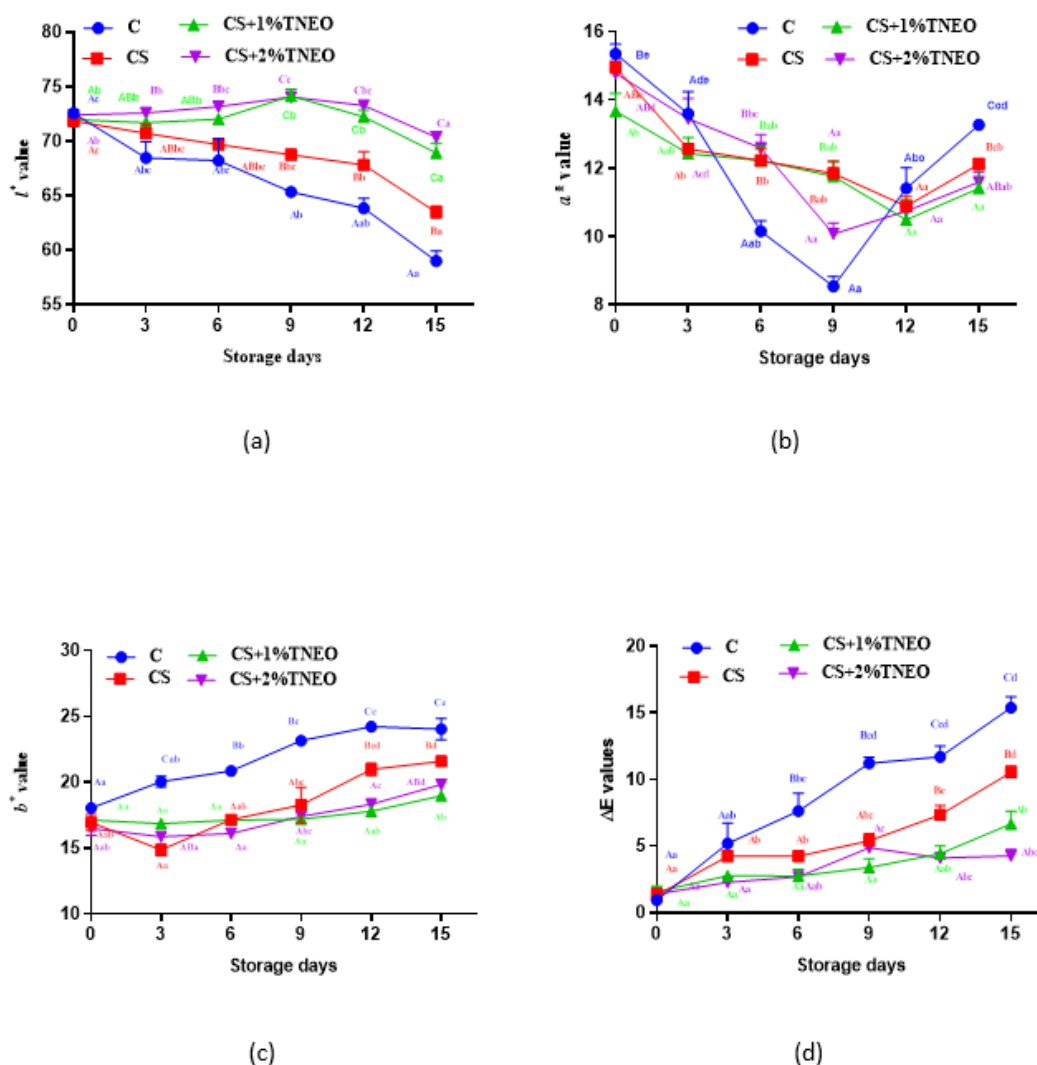


Figure 7. Color analysis of chicken drumsticks under refrigeration storage for 15 days; (a) l^* value; (b) a^* value; (c) b^* value; (d) ΔE value; C = chicken drumstick without any wrapping; CS = chicken drumstick wrapped with chitosan film; CS + 1% TNEO = chicken drumstick wrapped with chitosan film with a 1% thyme nanoemulsion; CS + 2% TNEO = chicken drumstick wrapped with a 2% thyme nanoemulsion.

3.15. Color analysis of the meat

Color stability is a paramount quality attribute in fresh meat, directly influencing consumer purchasing decisions. The impact of the bioactive films on the color parameters (l^* , a^* , b^* and ΔE) of chicken drumsticks throughout storage is detailed in Figure 7. A significant decrease in lightness (l^*) was observed in the no-chitosan (C) and chitosan-only (CS) drumstick samples, indicating surface darkening. In contrast, treatments (CS with 1% TNEO and CS with 2% TNEO) maintained or even increased brightness until day 9, likely due to light-scattering effects from the nanoemulsion droplets on the meat surface. This protective effect diminished in the final storage stage as spoilage progressed, although at a slower rate than that in the non-chitosan-packed sample.

The redness (a^* value), which is governed primarily by myoglobin, decreased significantly in all the samples over time because of oxidative processes. However, this decline was markedly slower ($p < 0.05$) in the treated samples. The sample with no chitosan packaging presented a terminal spike in the a^* value, a phenomenon often linked to advanced spoilage involving microbial protein degradation and lipid oxidation, which was effectively suppressed by the bioprotective films. This aligns with findings from Wang et al. [51] in chilled lambs in which thyme microcapsules were added to a biocomposite film.

Conversely, yellowness (b^* value) increased in all the samples, with the most pronounced change observed in the sample with no chitosan packaging (from 18.03 to 24.04). The CS + 1% TNEO and CS + 2% TNEO treatment samples presented the least variation, with final values of 18.97 and 19.82, respectively. The slightly higher b^* value in the CS + 2% TNEO-packed sample reflects the inherent yellowness of the thyme nanoemulsion, yet its minimal overall increase indicates the film's efficacy as a color protectant against spoilage-induced discoloration. Parallel findings have been reported in different studies [58,74], where the effects of different essential oils were determined on the basis of their potent color retention activity in muscle foods.

The overall color change (ΔE) was significantly lower in the treated (CS + 1% TNEO and CS + 2% TNEO) samples than in the samples with no chitosan film. The substantial discoloration in untreated meat signifies unchecked lipid peroxidation and microbial growth. In contrast, the sustained release of active compounds from the thyme nanoemulsion films successfully preserved the color and aesthetic value of the meat, thereby extending the shelf-life and marketability of the product, findings that are consistent with other studies on essential oil-based coatings [12,74].

4. Conclusions

This study demonstrated that incorporating thyme essential oil nanoemulsions into chitosan-based films markedly improved their functional properties, including UV and moisture barrier capacity, flexibility, and structural stability, making them suitable for active meat packaging applications. The films containing the 2% thyme nanoemulsion exhibited pronounced antimicrobial activity against *Staphylococcus aureus* and *Escherichia coli* and showed notable antioxidant potential, confirming the efficacy of the encapsulated bioactive compounds. When used to wrap raw chicken drumsticks stored under refrigeration, the 2% nanoemulsion film significantly delayed microbial spoilage, reduced lipid oxidation, and better preserved color attributes over 15 days than did the control samples without chitosan. These findings indicate that chitosan–thyme essential oil nanoemulsion films offer a promising green packaging strategy for extending the shelf-life and safety of raw poultry, with potential for application to other perishable muscle food and food products.

Supplementary

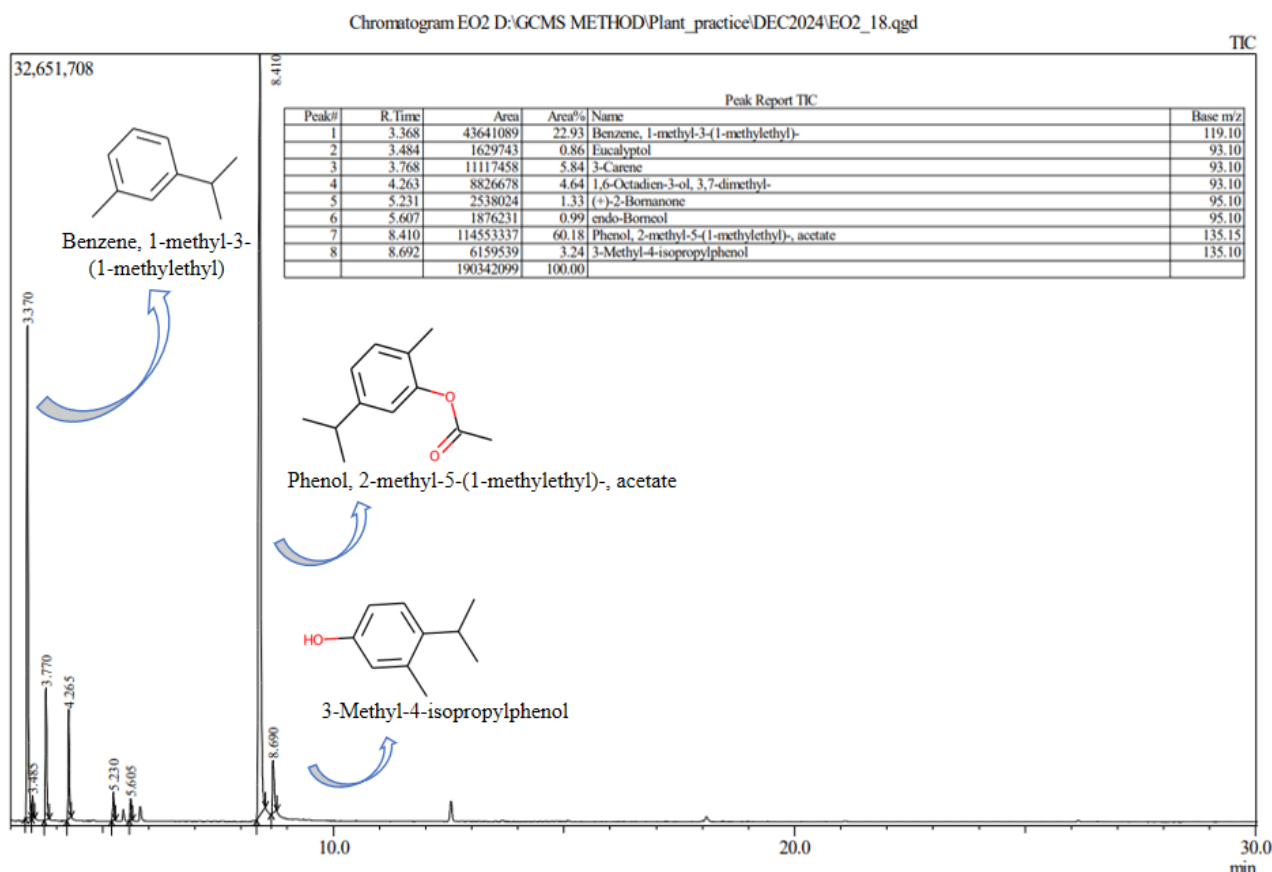


Figure SF 1. Gas chromatography and mass spectrometry analysis of thyme (*Thymus vulgaris*) essential oil with major identified bioactive components.

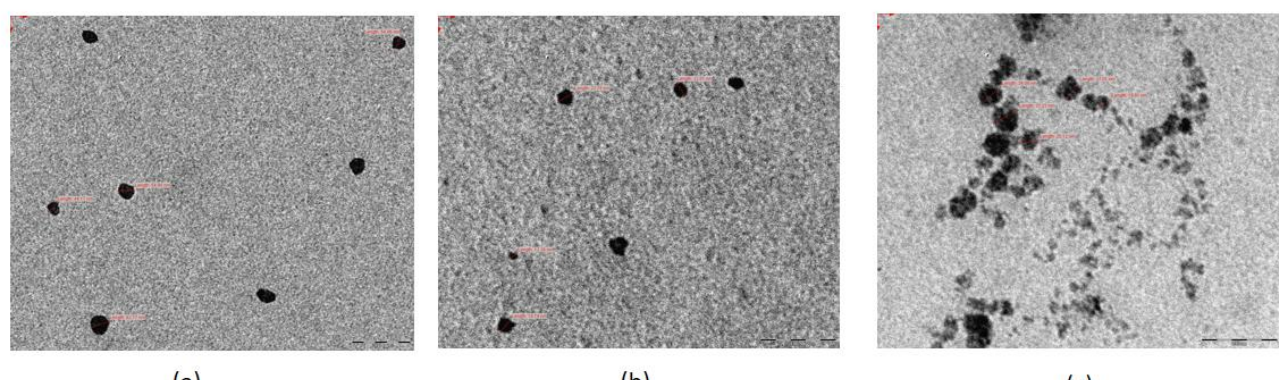


Figure SF 2. Transmission electron microscopy (TEM) image of the thyme oil nanoemulsion. (a): Thyme oil nanoemulsion (0.5%), (b): Thyme oil nanoemulsion (1.0%), (c): Thyme oil nanoemulsion (2.0%).

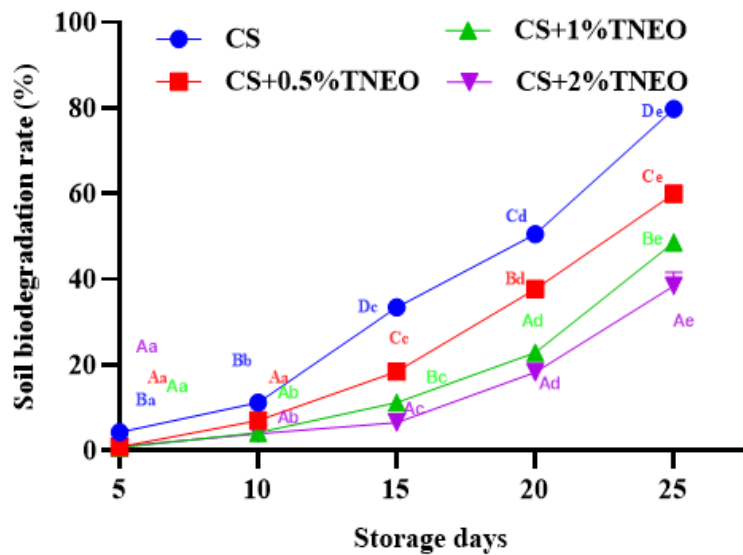


Figure SF 3. Soil biodegradation rates (%) of chitosan film (CS), chitosan film with 0.5% thyme oil nanoemulsion (CS + 0.5% TNEO), chitosan film with 1% thyme oil nanoemulsion (CS + 1% TNEO), and chitosan film with 2% thyme oil nanoemulsion (CS + 2% TNEO) during a 25-day trial.

Use of AI tools declaration

The authors declare that they have not used artificial intelligence (AI) tools in the creation of this article.

Acknowledgments

The authors wish to thank Banaras Hindu University (BHU), Varanasi, for supporting this research through the award of a SEED grant (21106) to the first author. The authors are also thankful to the Indian Institute of Technology (IIT), Varanasi, for providing facilities at the Central Instrumentation Facility (CIF), facilitating nanoemulsion characterization.

Author Contributions

D.B., P.P.K. and A.K.D. conceived, designed, and supervised the research. D.K., P.K.N., A.D., K.S., S.K., and A.S.P. performed different parts of the experimental work. A.K. carried out the statistical analysis. D.B. and A. K. D. prepared the initial draft of the manuscript. P.K.N. and A.K.D. reviewed and edited the manuscript.

Conflict of interest

The authors declare that they have no conflicts of interest.

References

1. Atarés L, Chiralt A (2016) Essential oils as additives in biodegradable films and coatings for active food packaging. *Trends Food Sci Technol* 48: 51–62. <https://doi.org/10.1016/j.tifs.2015.12.001>
2. Das A, Biswas S, Satyaprakash K, et al. (2025) Exploring the synergistic effects of plant powders and essential oil combination on the quality, and structural integrity of chicken sausages during storage. *Discov Food* 5: 336. <https://doi.org/10.1007/s44187-025-00615-z>
3. Aminzare M, Moniri R, Hassanzad Azar H, et al. (2022) Evaluation of antioxidant and antibacterial interactions between resveratrol and eugenol in carboxymethyl cellulose biodegradable film. *Food Sci Nutr* 10: 155–168. <https://doi.org/10.1002/fsn3.2656>
4. Kokkosi EK, Mylonaki EN, Karabagias VK, et al. (2024) Shelf life extension of Gyros" pork meat using plant extracts with antioxidant and antimicrobial activities. *Food Biosci* 62: 105542. <https://doi.org/10.1016/j.fbio.2024.105542>
5. Grande-Tovar CD, Serio A, Delgado-Ospina J, et al. (2018) Chitosan films incorporated with *Thymus capitatus* essential oil: mechanical properties and antimicrobial activity against degradative bacterial species isolated from tuna (*Thunnus* sp.) and swordfish (*Xiphias gladius*). *J Food Sci Technol* 55: 4256–4265. <https://doi.org/10.1007/s13197-018-3364-y>
6. Ozogul Y, Kuley Boğa E, Akyol I, et al. (2020) Antimicrobial activity of thyme essential oil nanoemulsions on spoilage bacteria of fish and food-borne pathogens. *Food Biosci* 36: 100635. <https://doi.org/10.1016/j.fbio.2020.100635>
7. Sun J, Pan X, Wang T, et al. (2025) Preparation, characterization and application of chitosan/thyme essential oil composite film. *Sci Rep* 15: 7934. <https://doi.org/10.1038/s41598-025-92267-3>
8. Das JK, Chatterjee N, Nanda PK, et al. (2024) Encapsulation and delivery of clove essential oil using nanoemulsions: Impact on the physicochemical, microbial, and sensory properties of chicken meatballs. *Food Biophys* 19: 701–716. <https://doi.org/10.1007/s11483-024-09861-7>
9. Das AK, Nanda PK, Bandyopadhyay S, et al. (2020) Application of nanoemulsion-based approaches for improving the quality and safety of muscle foods: A comprehensive review. *Compr Rev Food Sci Food Saf* 19: 2677–2700. <https://doi.org/10.1111/1541-4337.12604>
10. McClements DJ, Das AK, Dhar P, et al. (2021) Nanoemulsion-based technologies for delivering natural plant-based antimicrobials in foods. *Front Sustain Food Syst* 5: 643208. <https://doi.org/10.3389/fsufs.2021.643208>
11. Silva SB da, De Souza D, Lacerda LD (2019) Food applications of chitosan and its derivatives, *Chitin and Chitosan: Properties and Applications*, 315–347. <https://doi.org/10.1002/9781119450467.ch13>
12. Haghghi H, Gullo M, La China S, et al. (2021) Characterization of bio-nanocomposite films based on gelatin/polyvinyl alcohol blend reinforced with bacterial cellulose nanowhiskers for food packaging applications. *Food Hydrocoll* 113: 106454. <https://doi.org/10.1016/j.foodhyd.2020.106454>
13. Elshamy S, Khadizatul K, Uemura K, et al. (2021) Chitosan-based film incorporated with essential oil nanoemulsion foreseeing enhanced antimicrobial effect. *J Food Sci Technol* 58: 3314–3327. <https://doi.org/10.1007/s13197-020-04888-3>
14. Ojagh SM, Rezaei M, Razavi SH, et al. (2010) Development and evaluation of a novel biodegradable film made from chitosan and cinnamon essential oil with low affinity toward water. *Food Chem* 122: 161–166. <https://doi.org/10.1016/j.foodchem.2010.02.033>

15. Zehra A, Wani SM, Jan N, et al. (2022) Development of chitosan-based biodegradable films enriched with thyme essential oil and additives for potential applications in packaging of fresh collard greens. *Sci Rep* 12: 16923. <https://doi.org/10.1038/s41598-022-20751-1>
16. Haghghi H, Biard S, Bigi F, et al. (2019) Comprehensive characterization of active chitosan-gelatin blend films enriched with different essential oils. *Food Hydrocoll* 95: 33–42. <https://doi.org/10.1016/j.foodhyd.2019.04.019>
17. El-Sayed SM, El-Sayed HS (2021) Antimicrobial nanoemulsion formulation based on thyme (*Thymus vulgaris*) essential oil for UF labneh preservation. *J Mater Res Technol* 10: 1029–1041. <https://doi.org/10.1016/j.jmrt.2020.12.073>
18. Sheerzad S, Khorrami R, Khanjari A, et al. (2024) Improving chicken meat shelf-life: Coating with whey protein isolate, nanochitosan, bacterial nanocellulose, and cinnamon essential oil. *LWT* 197: 115912. <https://doi.org/10.1016/j.lwt.2024.115912>
19. Elsherief MF, Devecioglu D, Saleh MN, et al. (2024) Chitosan/alginate/pectin biopolymer-based Nanoemulsions for improving the shelf life of refrigerated chicken breast. *Int J Biol Macromol* 264: 130213. <https://doi.org/10.1016/j.ijbiomac.2024.130213>
20. Sayadi M, Abedi E, Oliyaei N (2025) Effect of Persian gum-gelatin based-pickering emulsion film loaded with Thyme essential oil on the storage quality of Barred mackerel (*Scomberomorus commerson*) fillet. *LWT* 215: 117241. <https://doi.org/10.1016/j.lwt.2024.117241>
21. Venkatesan R, Alrashed MM, Vetcher AA, et al. (2025) Next-generation food packaging: progress and challenges of biopolymer-based materials. *Polymers (Basel)* 17: 2299. <https://doi.org/10.3390/polym17172299>
22. Xu C, Xin Z, Yu R, et al. (2025) The control strategies for *E. coli* O157:H7 in food processing at the physical, chemical and biological levels. *Front Microbiol* 16: 1598090. <https://doi.org/10.3389/fmicb.2025.1598090>
23. Das AK, Nanda PK, Das A, et al. (2019) Hazards and safety issues of meat and meat products, *Food Safety and Human Health*, Elsevier Academic Press, 145–168. <https://doi.org/10.1016/B978-0-12-816333-7.00006-0>
24. Salimnejhad Z, Hassanzadazar H, Aminzare M (2023) Epinecidin-1 (an active marine antimicrobial peptide): Effects on the survival of inoculated *Escherichia Coli* O157:H7 and *Staphylococcus aureus* bacteria, antioxidant, and sensory attributes in raw milk. *Food Sci Nutr* 11: 5573–5581. <https://doi.org/10.1002/fsn3.3514>
25. Noori S, Zeynali F, Almasi H (2018) Antimicrobial and antioxidant efficiency of nanoemulsion-based edible coating containing ginger (*Zingiber officinale*) essential oil and its effect on safety and quality attributes of chicken breast fillets. *Food Control* 84: 312–320. <https://doi.org/10.1016/j.foodcont.2017.08.015>
26. Almasi L, Radi M, Amiri S, et al. (2021) Fabrication and characterization of antimicrobial biopolymer films containing essential oil-loaded microemulsions or nanoemulsions. *Food Hydrocoll* 117: 106733. <https://doi.org/10.1016/j.foodhyd.2021.106733>
27. Norcino LB, Mendes JF, Natarelli CVL, et al. (2020) Pectin films loaded with copaiba oil nanoemulsions for potential use as bio-based active packaging. *Food Hydrocoll* 106: 105862. <https://doi.org/10.1016/j.foodhyd.2020.105862>
28. Ferreira RR, Souza AG, Rosa DS (2021) Essential oil-loaded nanocapsules and their application on PBAT biodegradable films. *J Mol Liq* 337: 116488. <https://doi.org/10.1016/j.molliq.2021.116488>

29. Xavier LO, Sganzerla WG, Rosa GB, et al. (2021) Chitosan packaging functionalized with Cinnamodendron dinisii essential oil loaded zein: A proposal for meat conservation. *Int J Biol Macromol* 169: 183–193. <https://doi.org/10.1016/j.ijbiomac.2020.12.093>
30. Nisar T, Wang ZC, Yang X, et al. (2018) Characterization of citrus pectin films integrated with clove bud essential oil: Physical, thermal, barrier, antioxidant and antibacterial properties. *Int J Biol Macromol* 106: 670–680. <https://doi.org/10.1016/j.ijbiomac.2017.08.068>
31. Ghani S, Barzegar H, Noshad M, et al. (2018) The preparation, characterization and in vitro application evaluation of soluble soybean polysaccharide films incorporated with cinnamon essential oil nanoemulsions. *Int J Biol Macromol* 112: 197–202. <https://doi.org/10.1016/j.ijbiomac.2018.01.145>
32. He J, Zhang W, Goksen G, et al. (2024) Functionalized sodium alginate composite films based on double-encapsulated essential oil of wampee nanoparticles: A green preservation material. *Food Chem X* 24: 101842. <https://doi.org/10.1016/j.fochx.2024.101842>
33. Haridevamuthu B, Raj D, Chandran A, et al. (2024) Sustainable food packaging: Harnessing biowaste of *Terminalia catappa* L. for chitosan-based biodegradable active films for shrimp storage. *Carbohydr Polym* 329: 121798. <https://doi.org/10.1016/j.carbpol.2024.121798>
34. Nxumalo KA, Fawole OA, Aremu AO (2023) Development of chitosan-based active films with medicinal plant extracts for potential food packaging applications. *Processes* 12: 23. <https://doi.org/10.3390/pr12010023>
35. Almasi H, Azizi S, Amjadi S (2020) Development and characterization of pectin films activated by nanoemulsion and Pickering emulsion stabilized marjoram (*Origanum majorana* L.) essential oil. *Food Hydrocoll* 99: 105338. <https://doi.org/10.1016/j.foodhyd.2019.105338>
36. Ballester-Costa C, Sendra E, Fernández-López J, et al. (2016) Evaluation of the antibacterial and antioxidant activities of chitosan edible films incorporated with organic essential oils obtained from four Thymus species. *J Food Sci Technol* 53: 3374–3379. <https://doi.org/10.1007/s13197-016-2312-y>
37. Rahim A, Rostianti, Alam N, et al. (2023) Physicochemical and sensory characteristics of edible films from phosphorylated arenga starches using sodium tripolyphosphate. *IOP Conf Ser Earth Environ Sci* 1253: 012126. <https://doi.org/10.1088/1755-1315/1253/1/012126>
38. APHA (2015) Compendium of methods for the microbiological examination of foods. *Compend Methods Microbiol Exam Foods*.
39. Das A, Biswas S, Satyaprakash K, et al. (2024) Ratanjot (*Alkanna tinctoria* L.) root extract, rich in antioxidants, exhibits strong antimicrobial activity against foodborne pathogens and is a potential food preservative. *Foods* 13: 2254. <https://doi.org/10.3390/foods13142254>
40. Witte VC, KRAUSE GF, Bailey MEF (1970) A new extraction method for determining 2-thiobarbituric acid values of pork and beef during storage. *J Food Sci* 35: 582–585. <https://doi.org/10.1111/j.1365-2621.1970.tb04815.x>
41. Kowalczyk A, Przychodna M, Sopata S, et al. (2020) Thymol and thyme essential oil—New insights into selected therapeutic applications. *Molecules* 25: 4125. <https://doi.org/10.3390/molecules25184125>
42. Marchese A, Arciola C, Barbieri R, et al. (2017) Update on monoterpenes as antimicrobial agents: a particular focus on p-cymene. *Materials (Basel)* 10: 947. <https://doi.org/10.3390/ma10080947>
43. Keykhosravy K, Khanzadi S, Hashemi M, et al. (2020) Chitosan-loaded nanoemulsion containing Zataria Multiflora Boiss and Bunium persicum Boiss essential oils as edible coatings: Its impact on microbial quality of turkey meat and fate of inoculated pathogens. *Int J Biol Macromol* 150: 904–913. <https://doi.org/10.1016/j.ijbiomac.2020.02.092>

44. Amiri E, Aminzare M, Azar HH, et al. (2019) Combined antioxidant and sensory effects of corn starch films with nanoemulsion of *Zataria multiflora* essential oil fortified with cinnamaldehyde on fresh ground beef patties. *Meat Sci* 153: 66–74. <https://doi.org/10.1016/j.meatsci.2019.03.004>

45. Gupta P, Preet S, Ananya, et al. (2022) Preparation of *Thymus vulgaris* (L.) essential oil nanoemulsion and its chitosan encapsulation for controlling mosquito vectors. *Sci Rep* 12: 4335. <https://doi.org/10.1038/s41598-022-07676-5>

46. Liu J, Song F, Chen R, et al. (2022) Effect of cellulose nanocrystal-stabilized cinnamon essential oil Pickering emulsions on structure and properties of chitosan composite films. *Carbohydr Polym* 275: 118704. <https://doi.org/10.1016/j.carbpol.2021.118704>

47. Qin C, Li Z, Zhang J, et al. (2024) Preparation, physicochemical properties, antioxidant, and antibacterial activities of quaternized hawthorn pectin films incorporated with thyme essential oil. *Food Packag Shelf Life* 41: 101235. <https://doi.org/10.1016/j.fpsl.2023.101235>

48. Muñoz-Núñez C, Hevilla V, Zágora J, et al. (2025) Functionalization of chitosan-chitin nanowhiskers films by impregnation with essential oils via supercritical CO₂. *J Polym Environ* 33: 96–111. <https://doi.org/10.1007/s10924-024-03413-3>

49. Dey SC, Al-Amin M, Rashid TU, et al. (2016) Preparation, characterization and performance evaluation of chitosan as an adsorbent for remazol red. *Int J Latest Res Eng Technol* 2: 52–62.

50. Weerapol Y, Manmuan S, Chuenbarn T, et al. (2023) Nanoemulsion-based orodispersible film formulation of guava leaf oil for inhibition of oral cancer cells. *Pharmaceutics* 15: 2631. <https://doi.org/10.3390/pharmaceutics15112631>

51. Wang J, Li L, Li Y, et al. (2025) Characterization of thyme essential oil microcapsules and potato starch/pectin composite films and their impact on the quality of chilled mutton. *Food Chem* 464: 141692. <https://doi.org/10.1016/j.foodchem.2024.141692>

52. Li Z, Jiang X, Huang H, et al. (2022) Chitosan/zein films incorporated with essential oil nanoparticles and nanoemulsions: Similarities and differences. *Int J Biol Macromol* 208: 983–994. <https://doi.org/10.1016/j.ijbiomac.2022.03.200>

53. Sedlářková J, Janalíková M, Rudolf O, et al. (2019) Chitosan/thyme oil systems as affected by stabilizing agent: Physical and antimicrobial properties. *Coatings* 9: 165. <https://doi.org/10.3390/coatings9030165>

54. Aziz SB, Abdulwahid RT, Rasheed MA, et al. (2017) Polymer blending as a novel approach for tuning the SPR peaks of silver nanoparticles. *Polymers (Basel)* 9: 486. <https://doi.org/10.3390/polym9100486>

55. Qiao C, Ma X, Wang X, et al. (2021) Structure and properties of chitosan films: Effect of the type of solvent acid. *LWT* 135: 109984. <https://doi.org/10.1016/j.lwt.2020.109984>

56. Zhao R, Guan W, Zhou X, et al. (2022) The physicochemical and preservation properties of anthocyanidin/chitosan nanocomposite-based edible films containing cinnamon-perilla essential oil pickering nanoemulsions. *LWT* 153: 112506. <https://doi.org/10.1016/j.lwt.2021.112506>

57. Woźniak M, Młodziejewska J, Stefanowska K, et al. (2024) Chitosan-based films with essential oil components for food packaging. *Coatings* 14: 830. <https://doi.org/10.3390/coatings14070830>

58. Liu T, Liu L (2020) Fabrication and characterization of chitosan nanoemulsions loading thymol or thyme essential oil for the preservation of refrigerated pork. *Int J Biol Macromol* 162: 1509–1515. <https://doi.org/10.1016/j.ijbiomac.2020.07.207>

59. Carvalho RA, de Oliveira ACS, Santos TA, et al. (2020) WPI and cellulose nanofibres bio-nanocomposites: Effect of thyme essential oil on the morphological, mechanical, barrier and optical properties. *J Polym Environ* 28: 231–241. <https://doi.org/10.1007/s10924-019-01598-6>

60. Rahman L, Goswami J, Choudhury D (2022) Assessment of physical and thermal behaviour of chitosan-based biocomposites reinforced with leaf and stem extract of *Tectona grandis*. *Polym Polym Compos* 30: 1–12. <https://doi.org/10.1177/09673911221076305>

61. Luna PBFG da S de, Caetano VF, Andrade MF de, et al. (2024) Effect of thyme essential oil on the properties of poly (butylene adipate-co-terephthalate)(PBAT). *Polímeros* 34: e20240005. <https://doi.org/10.1590/0104-1428.20230009>

62. Mehdizadeh T, Tajik H, Razavi Rohani SM, et al. (2012) Antibacterial, antioxidant and optical properties of edible starch-chitosan composite film containing *Thymus kotschyanus* essential oil. *Vet Res forum an Int Q J* 3: 167–173.

63. Shen Z, Kamdem DP (2015) Development and characterization of biodegradable chitosan films containing two essential oils. *Int J Biol Macromol* 74: 289–296. <https://doi.org/10.1016/j.ijbiomac.2014.11.046>

64. Amiri H (2012) Essential oils composition and antioxidant properties of three thymus species. *Evidence-Based Complement Altern Med* 2012: 1–8. <https://doi.org/10.1155/2012/728065>

65. Al-Hilifi SA, Al-Ali RM, Petkoska AT (2022) Ginger essential oil as an active addition to composite chitosan films: Development and characterization. *Gels* 8: 327. <https://doi.org/10.3390/gels8060327>

66. Sani IK, Pirsa S, Tağı S (2019) Preparation of chitosan/zinc oxide/*Melissa officinalis* essential oil nano-composite film and evaluation of physical, mechanical and antimicrobial properties by response surface method. *Polym Test* 79: 106004. <https://doi.org/10.1016/j.polymertesting.2019.106004>

67. Peng Y, Li Y (2014) Combined effects of two kinds of essential oils on physical, mechanical and structural properties of chitosan films. *Food Hydrocoll* 36: 287–293. <https://doi.org/10.1016/j.foodhyd.2013.10.013>

68. Lian H, Shi J, Zhang X, et al. (2020) Effect of the added polysaccharide on the release of thyme essential oil and structure properties of chitosan based film. *Food Packag Shelf Life* 23: 100467. <https://doi.org/10.1016/j.fpsl.2020.100467>

69. Kanatt SR (2020) Development of active/intelligent food packaging film containing *Amaranthus* leaf extract for shelf life extension of chicken/fish during chilled storage. *Food Packag Shelf Life* 24: 100506. <https://doi.org/10.1016/j.fpsl.2020.100506>

70. Latif S, Ahmed M, Ahmed M, et al. (2024) Development of *Plumeria alba* extract supplemented biodegradable films containing chitosan and cellulose derived from bagasse and corn cob waste for antimicrobial food packaging. *Int J Biol Macromol* 266: 131262. <https://doi.org/10.1016/j.ijbiomac.2024.131262>

71. Khorshidi S, Mehdizadeh T, Ghorbani M (2021) The effect of chitosan coatings enriched with the extracts and essential oils of *Elettaria Cardamomum* on the shelf-life of chicken drumsticks vacuum-packaged at 4 °C. *J Food Sci Technol* 58: 2924–2935. <https://doi.org/10.1007/s13197-020-04794-8>

72. Huang M, Wang H, Xu X, et al. (2020) Effects of nanoemulsion-based edible coatings with composite mixture of rosemary extract and ϵ -poly-l-lysine on the shelf life of ready-to-eat carbonado chicken. *Food Hydrocoll* 102: 105576. <https://doi.org/10.1016/j.foodhyd.2019.105576>

73. Kamkar A, Molaei-aghaee E, Khanjari A, et al. (2021) Nanocomposite active packaging based on chitosan biopolymer loaded with nano-liposomal essential oil: Its characterizations and effects on microbial, and chemical properties of refrigerated chicken breast fillet. *Int J Food Microbiol* 342: 109071. <https://doi.org/10.1016/j.ijfoodmicro.2021.109071>
74. Wang W, Zhao D, Xiang Q, et al. (2021) Effect of cinnamon essential oil nanoemulsions on microbiological safety and quality properties of chicken breast fillets during refrigerated storage. *LWT* 152: 112376. <https://doi.org/10.1016/j.lwt.2021.112376>



AIMS Press

© 2025 the Author(s), licensee AIMS Press. This is an open access article distributed under the terms of the Creative Commons Attribution License (<http://creativecommons.org/licenses/by/4.0>)